

2023

Targeting the MIF-CD74 axis to overcome resistance to tyrosine kinase inhibitors in lung cancer

<https://hdl.handle.net/2144/48295>

"Downloaded from OpenBU. Boston University's institutional repository."

BOSTON UNIVERSITY

ARAM V. CHOBANIAN & EDWARD AVEDISIAN SCHOOL OF MEDICINE

Thesis

**TARGETING THE MIF-CD74 AXIS TO OVERCOME RESISTANCE
TO TYROSINE KINASE INHIBITORS IN LUNG CANCER**

by

MEGHAN LEE

B.S., Boston College, 2019

Submitted in partial fulfillment of the
requirements for the degree of
Master of Science

2023

© 2023 by
MEGHAN LEE
All rights reserved

Approved by

First Reader

Jean L. Spencer, Ph.D.
Instructor of Biochemistry

Second Reader

Susumu Kobayashi, Ph.D.
Associate Professor of Medicine

DEDICATION

I would like to dedicate this work to my family and friends who have supported me along
the way.

ACKNOWLEDGMENTS

Thank you to Dr. Ikei Koyabashi and Dr. Daisuke Shibahara for teaching me how to run experiments in the lab, and thank you to Dr. Motohiro Izumi for your wisdom, patience, and guidance in running all the experiments. Thank you to Dr. Susumu Kobayashi for your mentorship and for giving me an opportunity to work in your lab.

**TARGETING THE MIF-CD74 AXIS TO OVERCOME RESISTANCE
TO TYROSINE KINASE INHIBITORS IN LUNG CANCER**

MEGHAN LEE

ABSTRACT

Development of tyrosine kinase inhibitors (TKIs) against oncogenic drivers has significantly improved survival of patients with oncogene-mutated non-small cell lung cancer (NSCLC). However, acquired resistance to TKIs emerges over time in essentially all patients who initially respond. Recent evidence suggests that drug-tolerant persister (DTP) cells, which survive and adapt to targeted therapies during an early phase of treatment, play an important role in the emergence of drug resistance. A previous study reported that cluster of differentiation 74 (CD74) expression is upregulated in epidermal growth factor receptor (EGFR)-mutated lung cancer after treatment with EGFR-TKIs and that CD74 can be one of the DTP cell markers. However, both the mechanism underlying CD74 expression and the role of CD74 in DTP cells remain unclear.

In the current study, an attempt was made to identify the mechanism using cell culture systems and transgenic mouse models. The results confirmed *CD74* upregulation at the messenger RNA (mRNA) level after treatments with TKIs in various oncogene-mutated cell lines, including those with *EGFR* mutations, *ROS1* fusions, and *ALK* fusions. The class II transactivator (CIITA), upstream of CD74, and tumor necrosis factor (TNF)- α expression were induced by treatments with TKIs in tumor cells, leading to an increase in CD74 expression. In addition, the results showed that treatments with TKIs enhance the autocrine secretion of macrophage migration inhibitory factor (MIF), a

ligand of CD74, from tumor cells. This implied that autocrine stimulation of CD74 signaling blocks apoptosis and causes emergence of DTP cells. To examine whether CD74 plays an important role in the emergence of resistance to TKIs *in vivo*, experiments were completed in which lung-specific *EGFR-L858R-T790M* transgenic mice were crossed with *Cd74* knockout mice. The results showed that complete deletion of CD74 overcomes or delays resistance to TKIs. Taken together, the results of this study suggest that the MIF-CD74 axis can be a novel target to overcome resistance in driver-mutated NSCLC.

TABLE OF CONTENTS

DEDICATION	iv
ACKNOWLEDGMENTS	v
ABSTRACT.....	vi
TABLE OF CONTENTS.....	viii
LIST OF TABLES	ix
LIST OF FIGURES	x
LIST OF ABBREVIATIONS.....	xiii
INTRODUCTION	1
METHODS	7
RESULTS	15
CD74 EXPRESSION IN DTP CELLS.....	15
MECHANISMS OF CD74 UPREGULATION	16
ROLE OF CD74 IN ANTI-APOPTOSIS.....	22
TARGETING MIF.....	27
CO-CULTURING MACROPHAGES WITH CANCER CELLS	31
TARGETING CD74 WITH ANTI-CD74-ADC	40
COMPLETE DELETION OF CD74 SUPPRESSES TKI RESISTANCE	45
DISCUSSION.....	47
BIBLIOGRAPHY.....	52
CURRICULUM VITAE.....	60

LIST OF TABLES

Table 1. Primers Used in Quantitative PCR	9
---	---

LIST OF FIGURES

Figure 1. scRNA-Seq Analysis of Osimertinib-Resistant Lines.....	3
Figure 2. <i>CD74</i> mRNA Expression in Various Cancer Cell Lines.....	16
Figure 3. <i>CIITA</i> and <i>CD74</i> Expression in qPCR and Western Blot	18
Figure 4. <i>TNF-α</i> mRNA Levels in H1975, HCC78, and PC9ER.....	20
Figure 5. Caspase Assay in H1975 Cells Treated With Osimertinib.....	23
Figure 6. <i>BCL2L1</i> mRNA Levels in H1975 and HCC78 Cancer Cells.....	25
Figure 7. NF- κ B Activity in H1975 Cells and KO Cells Treated With Osimertinib	27
Figure 8. ELISA Results of H1975 and HCC78 Measuring MIF.....	28
Figure 9. Caspase Activity of H1975 and HCC78 With TKIs and MIF Inhibitor.....	30
Figure 10. Western Blot Results of H1975/HCC78 Treated with TKIs and MIF Inhibitor	30
Figure 11. <i>CD74</i> mRNA Levels in H1975/HCC78 Treated with TKIs and MIF Inhibitor	31
Figure 12. <i>CXCL10</i> and <i>CCL22</i> mRNA Levels in M0, M1, and M2 Macrophages	33
Figure 13. <i>CXCL10</i> and <i>CCL22</i> mRNA Levels in M0 macrophages Treated with MIF	35
Figure 14. Collecting Co-Culturing Macrophages With Cancer Cell Conditioned Media	37
Figure 15. <i>CXCL10</i> and <i>CCL22</i> mRNA Levels in H1975 Treated with TKIs and 4-IPP	38
Figure 16. Cell Viability in H1975 Cells in Macrophage Conditioned Media.....	40

Figure 17. Cell Viability in H1975 Cells Treated With Osimertinib and Antibody 42

Figure 18. Apoptosis Assays in H1975, HCC78 and PC9 With TKIs and Antibody 43

Figure 19. Cd74 Knockout Suppresses Resistance to EGFR-TKIs In Vivo..... 46

LIST OF ABBREVIATIONS

4-IPP	4-iodo-6-phenylpyrimidine
ADC	antibody-drug conjugate
ALK	anaplastic lymphoma kinase
anti-CD74-ADC	MMAE-conjugated anti-CD74 antibody
Bcl-2.....	B-cell lymphoma 2
BCL2L1	Bcl-2-like 1
BCL-XL	B-cell lymphoma-extra large
CD74.....	cluster of differentiation 74
cDNA	complementary DNA
CIITA	class II major histocompatibility complex transactivator
CM	conditioned medium
DMSO.....	dimethyl sulfoxide
DOX.....	doxycycline
DTP	drug-tolerant persister
ECL.....	enhanced chemiluminescence
EGFR	epidermal growth factor receptor
ELISA	enzyme-linked immunosorbent assay
FBS	fetal bovine serum
GAPDH.....	glyeraldehyde-3-phosphate dehydrogenase
IC50.....	half-maximal inhibitory concentration
IFN- γ	interferon gamma

IgG1κ	immunoglobulin G1 kappa
IgGκ	immunoglobulin G kappa
IL	interleukin
iso	isotype
IgG1κ	immunoglobulin G1 kappa
KO	knockout
LPS	lipopolysaccharide
MHC	major histocompatibility complex
MIF	migration inhibitory factor
MMAE	monomethyl auristatin E
MRI	magnetic resonance imaging
mRNA	messenger RNA
NF	nuclear factor
NSCLC	non-small cell lung cancer
OR _x	osimertinib-resistant
osi	osimertinib
PBS	phosphate-buffered saline
PBST	phosphate-buffered saline with Tween
PC9ER	PC9-erlotinib resistant
PCR	polymerase chain reaction
PD	progressive disease
PE	phycoerythrin

PMA.....phorbol-12-myristate-13-acetate
PR.....partial response
PVDF.....polyvinylidene difluoride
qPCR..... quantitative polymerase chain reaction
RNA.....ribonucleic acid
ROS1.....c-ros oncogene 1
rpm..... revolutions per minute
RPMI..... Roswell Park Memorial Institute
RT-PCR.....reverse transcription polymerase chain reaction
scRNA-seq..... single-cell RNA sequencing
SD..... stable disease
SDS..... sodium dodecyl sulfate
T790M.....threonine-methionine change at position 790
TCA.....trichloroacetic acid
TKI..... tyrosine kinase inhibitor
TME..... tumor microenvironment
TNF..... tumor necrosis factor
VC-PAB..... valine-citrulline-aminobenzylcarbamate
WT..... wild type

INTRODUCTION

Despite improving therapeutics and advancements in research, still stands as one of the primary causes of cancer-related deaths (Cancer Statistics Center, n.d.). Lung cancer can be broadly classified into two categories, namely non-small cell lung cancer (NSCLC) and small cell lung cancer, with NSCLC making up about 80% of cases (American Lung Association, 2022). The available treatments for cancer are largely determined by the stage of the disease, as well as other considerations such as age, overall health status, and desired treatment outcomes. A range of treatment options are currently available, including chemotherapies, surgical interventions, targeted and immunotherapies, radiation therapy.

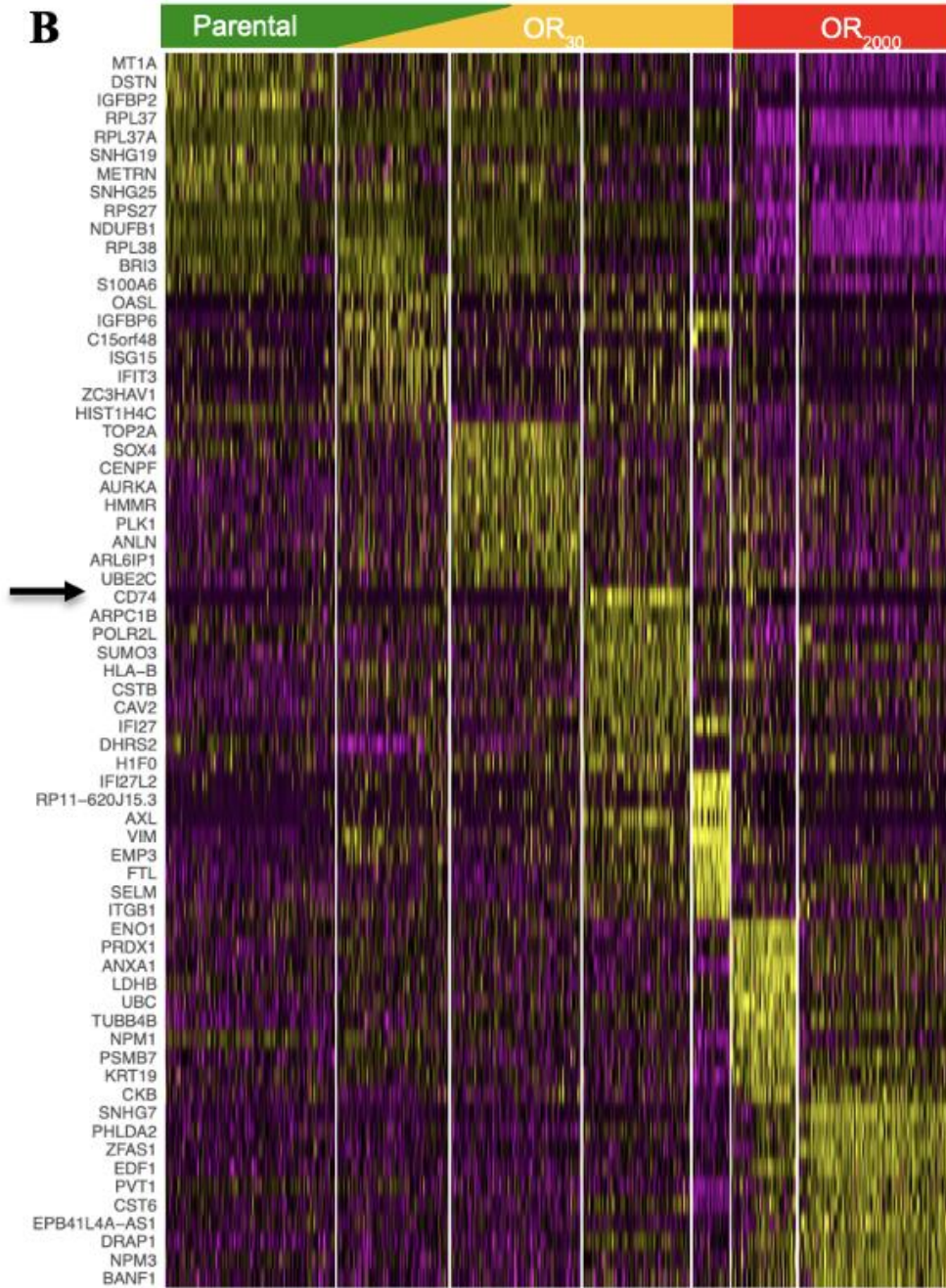
Targeted Therapies in Oncogenic-Mutated Cancer

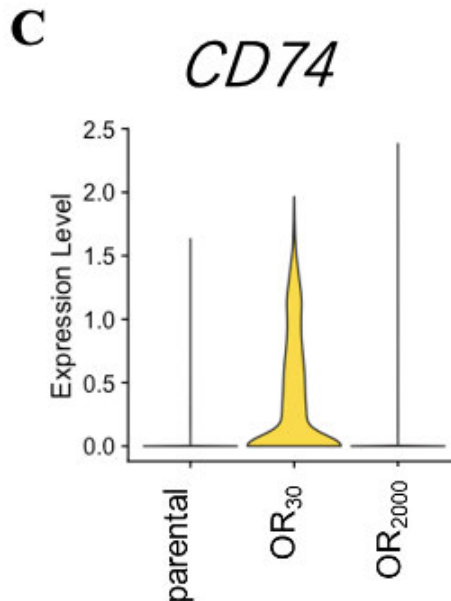
Advancements in genomic sequencing have led to the discovery of activating mutations such as epidermal growth factor receptor (EGFR), c-ros oncogene 1 (ROS1), and anaplastic lymphoma kinase (ALK) in NSCLC. The EGFR is a transmembrane glycoprotein with tyrosine kinase activity and its typical role is to participate in cell signaling pathways that regulate cell division and survival. Mutations to the EGFR can lead to tumorigenesis because of inappropriate activation (Sigismund et al., 2018). First-generation tyrosine kinase inhibitors (TKIs), erlotinib and gefitinib, were developed and approved by the U.S. Food and Drug Administration in the early 2000s for NSCLC patients with EGFR mutations. Afatinib and dacomitinib were later approved as second-generation TKIs in 2013. Despite dramatic antitumor responses after treatment with first- and second-generation TKIs, almost all tumors acquired resistance within two years

(Gazdar, 2009; Kashima et al., 2021). Sequencing of these resistant tumors revealed the emergence after treatment of a threonine-to-methionine change at position 790 (T790M) of EGFR, otherwise known as a gatekeeper mutation (Kobayashi et al., 2005). This led to the development of the third-generation TKI osimertinib in 2015 for EGFR T790M mutation-positive NSCLC. Osimertinib is commonly employed as the initial therapeutic approach for NSCLC that presents with a positive EGFR mutation, whether or not the T790M is present (Ramalingam et al., 2018). Patients who received osimertinib treatment had longer progression-free survival but still acquired resistance over time (Soria et al., 2018). For ROS1-positive and ALK-positive patients, crizotinib and alectinib, respectively, are used as first-line treatment options, but resistance is also seen in both populations (Lin et al., 2021; Pan et al., 2021).

Drug-Tolerant Persister Cells

New investigations into mechanisms of resistance have revealed the existence of drug-tolerant persister (DTP) cells, which constitute a subpopulation capable of enduring and adapting to targeted therapies (Hata et al., 2016). DTP cells enter a persister state, which is characterized by slow proliferation and reduced drug sensitivity during drug treatment, allowing these cell subpopulations to survive long enough to acquire drug resistance by epigenetic and genetic alterations (Kashima et al., 2021; Mikubo et al., 2021). In addition, research has shown that there are diverse mechanisms of resistance that can arise from persister cells and contribute to intratumoral heterogeneity (Ramirez et al., 2016).





Note. (A) This panel presents t-Distributed Stochastic Neighbor Embedding plots based on single-cell sequencing of clusters in parental, low-resistance, and high-resistance H1975 cancer cells. A comparison of plots indicates a unique gene signature (red oval) in low-resistance cells (OR₃₀). (B) Transcription analyses show differential regulation of genes in varying cell states. The arrow denotes CD74, a potential DTP marker. Adapted from (Kashima et al., 2021). (C) Violin plot indicates CD74 expression in H1975 low-resistance cells. CD74 = cluster of differentiation 74; DTP = drug-tolerant persister cells; OR_x = osimertinib resistance at x nM; scRNA-seq = single-cell RNA sequencing.

In this report, Kashima et al. (2021) noticed that CD74 was induced by osimertinib as seen in increased messenger RNA (mRNA) and protein levels. The authors suggested that CD74 upregulation by osimertinib treatment promoted the DTP state by inducing anti-apoptotic proteins like B-cell lymphoma-extra large (BCL-XL), thereby inhibiting apoptosis. BCL-XL is a protein that is encoded by *BCL2L1*, a gene that is

associated with resistance to apoptosis, playing a major role in developing and maintaining DTP cells.

CD74 and MIF

CD74 is a transmembrane protein that is associated with class II major histocompatibility complex (MHC), which is important for the initiation of the antigen-specific immune response by presenting processed antigens (Holling et al., 2004). CD74 also acts as a cell surface receptor for the cytokine macrophage migration inhibitory factor (MIF), which contributes to cell survival and proliferation. The binding of MIF to CD74 induces the signaling cascade of ERK and PI3K/AKT (protein kinase B) pathways and the upregulation of pro-tumorigenic molecules (Tanese et al., 2015). It is widely recognized that CD74 is considerably overexpressed in various B-cell and myeloid cell cancers, such as myeloid leukemia, multiple myeloma, and diffuse large B-cell lymphoma, at both the ribonucleic acid (RNA) and protein level. (Abrahams et al., 2018; Ruvolo et al., 2019; Zhao et al., 2019). However, the mechanism of how CD74 maintains the DTP state in lung cancers is unknown.

Specific Aims

The specific aims of this study are:

1. To characterize the CD74 signaling pathway in DTP cells.
2. To evaluate the role of the tumor microenvironment (TME) on cancer cells.
3. To determine whether suppression of CD74 signaling can overcome resistance to TKIs using cell culture systems and transgenic mouse models.

METHODS

Cell Lines

NCI-H1975 (H1975) and HCC827 cells were purchased from the American Type Culture Collection (Manassas, VA, USA). PC9 cells were kindly provided by Dr. Pasi Jänne, HCC78 and H3122 cells were kindly provided by Dr. Hideo Watanabe, and THP-1 cells were kindly provided by Dr. Daniel Tenen. Erlotinib-resistant PC9 (PC9ER) cells were established by culturing each cell line with increasing concentrations of osimertinib (LC Laboratories, #O7200, 10 nmol/L to 2,000 nmol/L). All cell lines were grown in Roswell Park Memorial Institute (RPMI)-1640 medium (Corning, #MT10040CV) with 10% fetal bovine serum (FBS) (Corning, #35-010-CV), 100 µg/mL penicillin, and 100 units/mL streptomycin (Corning, #30-002-CI).

Generation of Stable Cell Lines

The generation of CD74 knockout (KO) in H1975 cells was previously reported (Kashima et al., 2021). H1975 CD74KO and control cells were transfected with nuclear factor (NF)-κB-reporter constructs or control constructs using the TransIT-X2 Dynamics Delivery System (Mirus, #MIR 6003). The pNL3.2. NF-κB-RE vector and pNL2.2 control vector were purchased from Promega. Stable cell lines (CD74KO-NF-κB-H1975 and Ctrl-NF-κB-H1975) were obtained by selection in 200 µg/mL hygromycin B (Sigma, #10843555001).

Quantitative Polymerase Chain Reaction (qPCR)

RNA was extracted and purified following the ZYMO instruction manual and using an RNA isolation kit (ZYMO Research Corp., Direct-zol RNA Miniprep Plus,

#R2072). RNA concentration and purity were measured using spectrophotometric absorbance (NanoDrop, ThermoFisher). Conversion of up to 2 µg of RNA to complementary DNA (cDNA) was carried out by means of the reverse transcription polymerase chain reaction (RT-PCR) using the High-Capacity cDNA Reverse Transcription Kit (Applied Biosystems, ThermoFisher Scientific, #4368814). Glyceraldehyde-3-phosphate dehydrogenase (GAPDH) expression levels were used as a control for varying RNA levels. Samples were prepared using iTaq Universal SYBR Green Supermix (Bio-Rad, #1725121), a fluorescent dye, and gene specific primers. The mRNA expression levels were measured using the Rotor Gene 6000 sequence detection system (Qiagen). The sequences of various primers used are summarized in **Table 1**.

Table 1*Primers Used in Quantitative PCR*

PRIMERS	DIRECTION	SEQUENCE (5' → 3')
<i>BCL2L1</i>	F	ATG GCA GCA GTA AAG CAA GC
	R	CGG AAG AGT TCA TTC ACT ACC TGT
<i>CIITA</i>	F	CCT GGA GCT TCT TAA CAG CGA
	R	TGT GTC GGG TTC TGA GTA GAG
<i>CCL22</i>	F	ATT ACG TCC GTT ACC GTC TG
	R	TAG GCT CTT CAT TGG CTC AG
<i>CD74</i>	F	CCA GCA TGG GCA GTT GCT CA
	R	GGA GAA GCA GGA GCT GTC GG
<i>CXCL10</i>	F	TGC CAT TCT GAT TTG CTG CC
	R	TGC AGG TAC AGC GTA CAG TT
<i>GAPDH</i>	F	CCA GGC GCC CAA TAC G
	R	CCA CAT CGC TCA GAC ACC AT
<i>MIF</i>	F	CGG ACA GGG TCT ACA TCA A
	R	CTT AGG CGA AGG TGG AGT T
<i>TNF-α</i>	F	CCT CTC TCT AAT CAG CCC TCT G
	R	GAG GAC CTG GGA GTA GAT GAG

Note. This table lists the various primers used in quantitative polymerase chain reaction (qPCR). Primers: BCL2L1 = Bcl-2-like 1; CIITA = class II major histocompatibility complex transactivator; CCL22 = chemokine ligand 22; CD74 = cluster of differentiation 74; CXCL10 = C-X-C motif chemokine 10; GAPDH = glyceraldehyde-3-phosphate dehydrogenase; MIF = migration inhibitory factor; TNF- α = tumor necrosis factor alpha. Direction: F = forward; R = reverse. Sequence: A = adenine; C = cytosine; G = guanine; T = thymine.

Western Blotting

For the preparation of cell pellets, growth medium was aspirated from culture plates, and cells were washed with phosphate-buffered saline (PBS). PBS contained 137 mM NaCl, 2.7 mM KCl, 10 mM Na₂HPO₄, and 1.8 mM KH₂PO₄ at pH 7.4. Trypsin (Gibco) was added to the dish (10% of medium volume), which was incubated at 37 °C

for 5 minutes to detach the cells from the plate. Once the cells were detached, growth medium was added to resuspend the cells, and the contents were transferred to a 1.7-mL microcentrifuge tube (Eppendorf) and centrifuged at 1,200 revolutions per minute (rpm) at 4 °C to collect the cell pellet.

Samples were prepared using the trichloroacetic acid (TCA) protein extraction method. The cell pellet was resuspended in 500 µL of 0.15 M NaCl solution, and a 50-µL volume of 100% TCA was added. The cells were then incubated on ice for 15 minutes. After incubation, the cells were centrifuged at 14,000 rpm for 5 minutes at 4 °C, and the supernatant was aspirated. Depending on the size of the pellet, a volume (50–200 µL) of 1x sodium dodecyl sulfate (SDS) buffer was added to the tube, and the cell pellet was broken down. A volume (1–4 µL) of 1M Tris hydrochloride at pH 7.5 was added until the mixture turned blue. The samples were sonicated and boiled at 95 °C for 3 minutes.

Samples were then run and separated on 6%–10% SDS polyacrylamide gels by gel electrophoresis and were transferred onto polyvinylidene difluoride (PVDF) membranes (Millipore, #IPVH00010). The membranes were blocked in 5% nonfat milk in phosphate-buffered saline with Tween (PBST) and incubated overnight with the following antibodies: anti-CD74 (Invitrogen, PA5-22113), anti-BCL-XL (Cell Signaling, #2764), anti-class II transactivator (CIITA) (Santa Cruz, #sc-13556), anti-β-actin (Cell Signaling, #4970). The membranes were then incubated for 2 hours with horseradish peroxidase-conjugated secondary mouse or rabbit antibodies in 5% nonfat milk and PBST. Signals were detected using enhanced chemiluminescence (ECL) Prime Western

Blotting Detection Reagent (ThermoFisher, #32106) and developed on an Amersham Imager 600 (GE Healthcare).

Apoptosis Assay

To evaluate apoptosis, caspase activity was determined using the Caspase-Glo 3/7 Assay System (Promega). In 96-well plates, 2,000 cells were seeded and incubated for 24 hours prior to the assay. They were then treated for another 24 or 48 hours with osimertinib, crizotinib, alectinib, anti-CD74 antibody, immunoglobulin G kappa (IgG κ) isotype, anti-CD74-antibody-drug conjugate (ADC), anti-isotype-ADC, or dimethyl sulfoxide (DMSO). Caspases-3 and -7 (caspase 3/7) activity was detected using SpectraMax iD3 (Molecular Devices). The results were measured as luminescence units which were obtained after subtracting the luminescence value of a blank reaction and dividing by cell number.

Flow Cytometric Analysis

H1975 cells were exposed to 100 nM osimertinib for a duration of 48 hours. After treatment, the cells were subjected to staining using mouse monoclonal antibodies labeled with phycoerythrin (PE) to detect CD74 (BioLegend, #326808) or mouse immunoglobulin G1 kappa (IgG1 κ) isotype control labeled with PE (BioLegend, #400114). The stained cells were then analyzed through flow cytometric analysis using a CytoFLEX LX Flow Cytometer (Beckman Coulter). CD74-positive or -negative cells were sorted. Gating was determined based on fluorescence intensity values and was done by an expert with experience in flow cytometry gating methods.

Reporter Assay

Stable cell lines (CD74KO-NF- κ B-H1975 and Ctrl-NF- κ B-H1975) (2,000 cells/mL) were incubated overnight and were treated with 30 nM osimertinib for another 24, 48, and 96 hours. Luciferase activity was measured using the Nano-Glo Luciferase Assay System (Promega, #N1110). Nano-luciferase activity was normalized to cell numbers.

Enzyme-Linked Immunosorbent Assay (ELISA)

The Human MIF Quantikine ELISA Kit (R&D Systems, #DMF00B) was utilized to quantify the secretion of MIF in the conditioned medium (CM) following the manufacturer's guidelines. The absorbance was recorded at 450 nm. The concentration detected in each sample was normalized to the total cellular protein per dish, and the findings were expressed as ng/ng protein.

Generation of Antibody-Drug Conjugate (ADC)

Humanized antihuman milatuzumab monoclonal antibody (anti-CD74 antibody) (MyBioSource, #MBS1563371) and human immunoglobulin G1 kappa (IgG1 κ) isotype (MedChemExpress, #HY-P99001) were purchased. Anti-CD74 antibody was labeled with monomethyl auristatin E (MMAE) using a valine-citrulline-aminobenzylcarbamate (VC-PAB) linker. MMAE-conjugated anti-CD74 antibody (anti-CD74-VC-PAB-MMAE; anti-CD74-ADC) and human IgG1 κ isotype (iso-VC-PAB-MMAE; iso-ADC) were prepared using a kit (CellMosaic Inc., #CM11409) and following the manufacturer's instructions.

Co-Culturing of Cancer Cells With Macrophages

THP-1 cells were treated with 150 nM phorbol-12-myristate-13-acetate (PMA) (LC Laboratories, #P-1680) for 24 hours and then incubated in RPMI (PMA-free) for an additional 24 hours to obtain M0 macrophages. M0 macrophages were then differentiated into M1 macrophages using 10 ng/mL lipopolysaccharide (Sigma, #L-3012) and 20 ng/mL interferon gamma (INF- γ) (Fisher Scientific, #PHC3021) for 24 hours. Alternatively, M0 macrophages were differentiated into M2 macrophages using 20 ng/mL interleukin (IL)-4 (R&D Systems, #204-IL) and 20 ng/mL IL-13 (R&D Systems, #213-ILB) for 96 hours.

Mice

Animal studies were approved by the Institutional Animal Care and Use Committee at Beth Israel Deaconess Medical Center (Boston, MA, USA). A previous study had generated *EGFR-L858R-T790M (EGFR^{TL})/CCSP-rtTA* bi-transgenic mice cohorts (Li et al., 2007). The *Cd74* knockout (KO) mice were purchased from The Jackson Laboratory (Bar Harbor, ME, USA). A *Cd74* KO lung cancer mouse model was established by crossing *EGFR^{TL}/CCSP-rtTA* mice with *Cd74* KO mice. Mouse genotypes were confirmed by PCR using appropriate primers. When male and female juvenile mice reached three to five weeks of age, they were treated with doxycycline (DOX) for eight to ten weeks. Immediately after DOX treatment, the mice underwent magnetic resonance imaging (MRI). Osimertinib was administered by oral gavage at five mg/kg/day, six days a week for two weeks, and then discontinued for two weeks while maintaining a DOX-containing diet. This cycle of “drug-on/drug-off” was repeated twice, followed by four

weeks of osimertinib treatment. Tumor growth was monitored by MRI after treatment with osimertinib for two weeks in each cycle. The lungs from these mice were dissected and subjected to histological analysis.

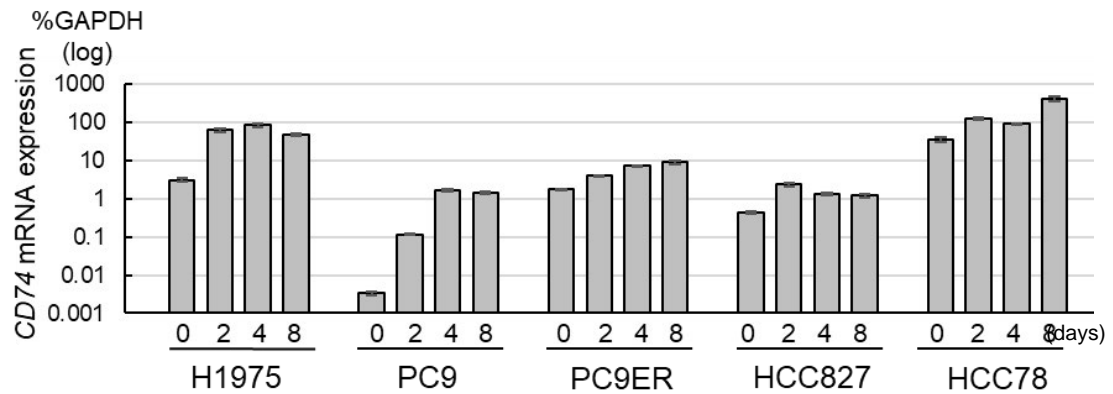
Statistical Analysis

Data were presented as the mean plus or minus the standard deviation and were analyzed with a *t*-test. Asterisks in figures indicated *p* values as follows: **p* < .05, ***p* < .005, or ns for no significance.

RESULTS

CD74 Expression in DTP Cells

Before the mechanism of CD74 in DTP cells was examined, observations were made of CD74 expression in various cancer cell lines treated with TKIs over a timed course. Cancer cell lines H1975, PC9, and HCC827 harbor EGFR mutations, HCC78 has a ROS1 rearrangement, and H3122 has ALK rearrangement. Thus, H1975, PC9, PC9ER, and HCC827 cell lines were treated with 100 nM osimertinib (EGFR inhibitor), HCC78 cells were treated with 3 μ M crizotinib (ROS1 inhibitor), and H3122 cells were treated with 100 nM alectinib (ALK inhibitor). A quantitative polymerase chain reaction (qPCR) was conducted to measure CD74 expression on days 0, 2, 4, and 8 of treatment. As seen in **Figure 2**, *CD74* mRNA expression was upregulated in samples treated with TKIs compared with day 0 in various lung cancer cell lines.

Figure 2*CD74 mRNA Expression in Various Cancer Cell Lines*

Note. This figure shows the qPCR results of *CD74* mRNA expression levels in various cancer cell lines on 0, 2, 4, and 8 days of treatment. Cell lines H1975, PC9, PC9ER, and HCC827 were treated with 100 nM osimertinib, HCC78 was treated with 3 μ M crizotinib, and H3122 was treated with 100 nM alectinib. Plotted values are means (with standard deviations). *CD74* = cluster of differentiation 74; *GAPDH* = glyceraldehyde-3-phosphate dehydrogenase; mRNA = messenger ribonucleic acid; qPCR = quantitative polymerase chain reaction; PC9ER = erlotinib-resistant PC9.

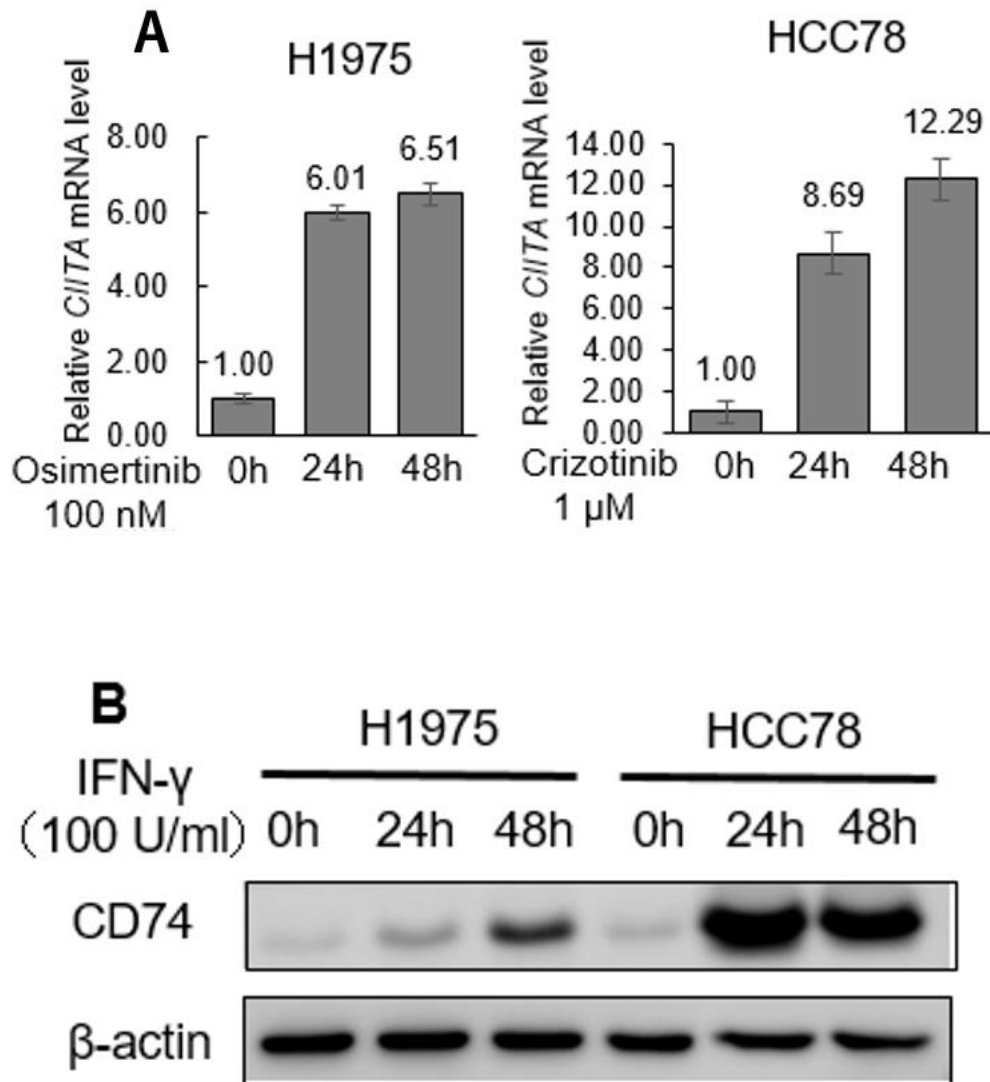
Mechanisms of CD74 Upregulation

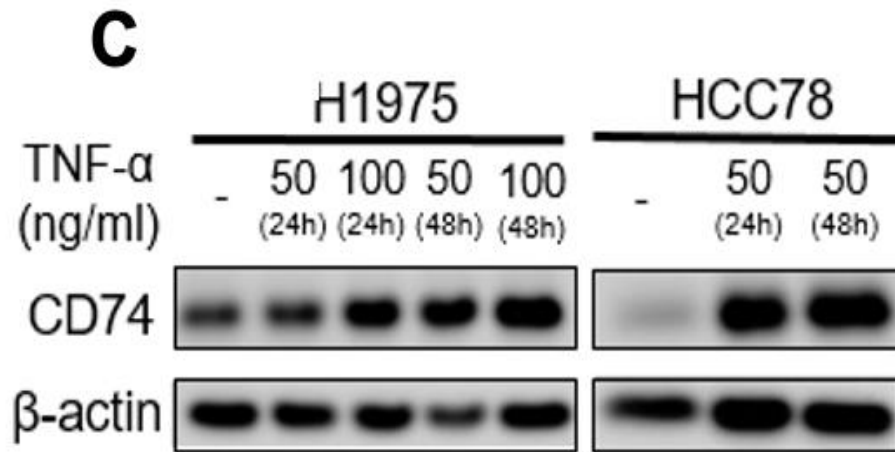
Experiments were completed to understand the different mechanisms that contribute to *CD74* upregulation. Cancer cells were first treated with TKIs and then evaluated for their effects on *CIITA*, which is upstream of *CD74* (Bruchez et al., 2020). *CIITA* is involved in regulating the activity of MHC class I and II genes, which are associated with the systemic immune response. *CIITA* is normally inhibited by EGFR signaling; therefore, when TKIs are used to inhibit EGFR, *CIITA* is no longer inhibited and can initiate a cascade promoting MHC class I and II promoters (Pollack et al., 2011). Interferon gamma ($\text{IFN-}\gamma$) is also involved in this pathway in that the $\text{IFN-}\gamma$ receptor

complex activates the *CIITA* promoter. Thus, H1975 and HCC78 cells were treated with 100 nM osimertinib and 1 μ M crizotinib, respectively, over the course of two days, and *CIITA* mRNA levels were measured by qPCR (**Figure 3A**). In both cell lines, *CIITA* mRNA levels were upregulated by day 1 of treatment with TKIs.

H1975 and HCC78 cells were also treated with IFN- γ (100 U/mL), and CD74 protein expression was determined by western blotting. In **Figure 3B**, there was increased expression of CD74 on days 1 and 2 of treatment with IFN- γ in H1975 and HCC78 cells. These results suggest that IFN- γ upregulated CD74 expression; however, an investigation of whether cancer cells released IFN- γ by autocrine secretion found no results by qPCR and ELISA.

H1975 and HCC78 cancer cells were then treated with tumor necrosis factor (TNF)- α (50 ng/mL and 100 ng/mL), and a western blot was conducted to look at CD74 expression. As seen in **Figure 3C**, CD74 expression increased with treatment of TNF- α in both cell lines.

Figure 3*CIITA and CD74 Expression in qPCR and Western Blot*

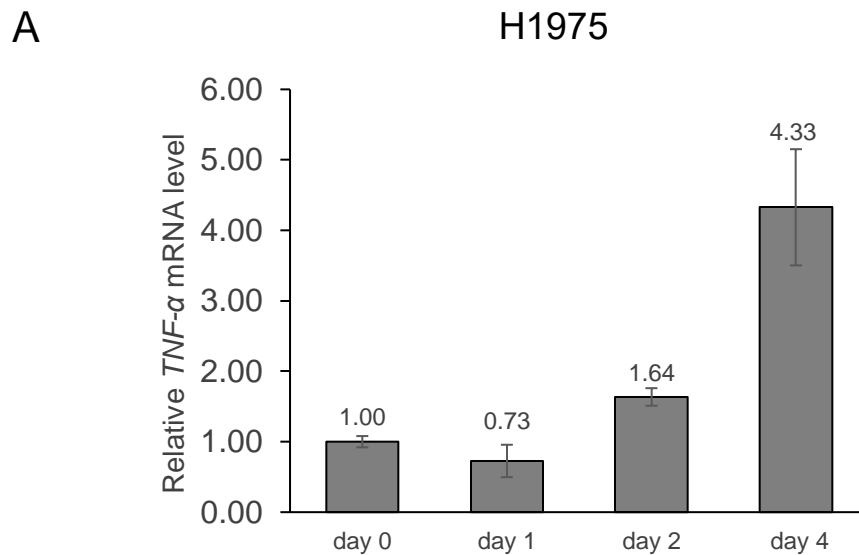


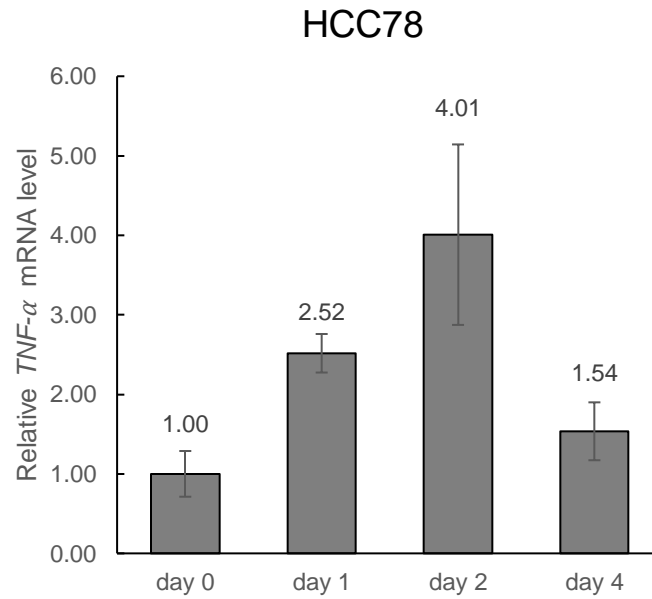
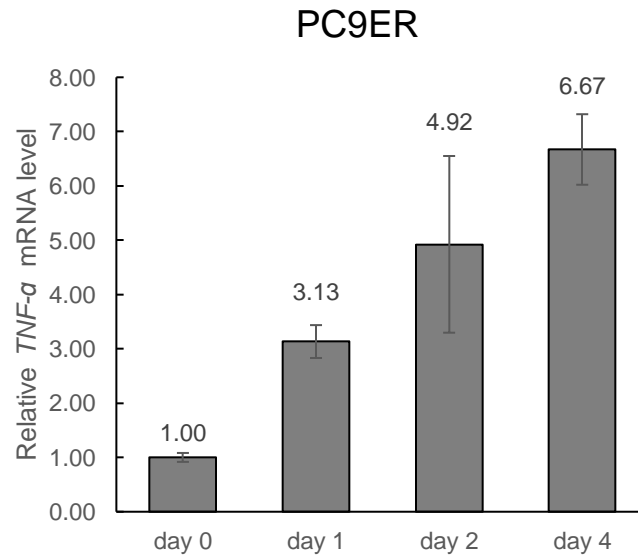
Note. This figure contains qPCR and western blot results for *CIITA* and CD74 expression in H1975 and HCC78 cell lines. (A) qPCR results show *CIITA* mRNA levels in H1975 and HCC78 cells when treated with 100 nM osimertinib and 1 μ M crizotinib, respectively. Plotted values are means (with standard deviations). (B) Western blot results show CD74 expression in H1975 and HCC78 cells when treated with 100 U/mL IFN- γ . (C) Western blot results show CD74 expression in H1975 and HCC78 cells when treated with TNF- α . β -actin = control for western blots; IFN- γ = interferon gamma; mRNA = messenger ribonucleic acid ; qPCR = quantitative polymerase chain reaction; TNF- α = tumor necrosis factor alpha.

The next experiments were done to determine if TNF- α was secreted from cancer cells by autocrine secretion. Over the course of four days, H1975 and PC9ER cancer cells were treated with 100 nM osimertinib, HCC78 cells were treated with 1 μ M crizotinib, and TNF- α was measured by qPCR. As seen in **Figure 4**, TNF- α mRNA levels increased when cancer cells were treated with TKIs, indicating that TNF- α was secreted from cancer cells in an autocrine manner. From these experiments, it appeared that CIITA upregulation by TKIs and treatment with TNF- α were related to upregulation of CD74 expression.

Figure 4

TNF- α mRNA Levels in H1975, HCC78, and PC9ER Cells

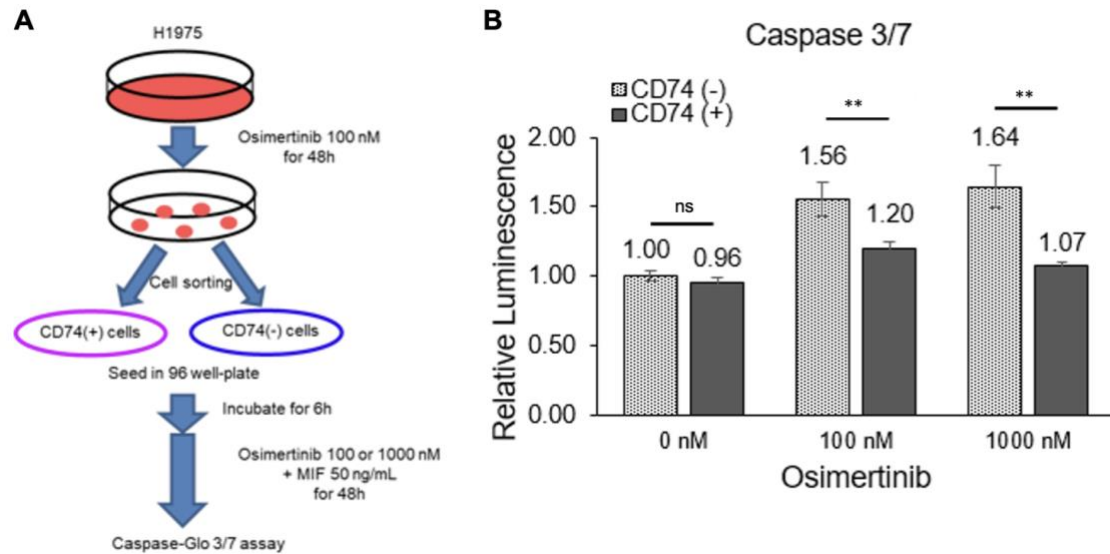


B**C**

Note. This figure shows the qPCR results for $TNF-\alpha$ mRNA levels in H1975, HCC78, and PC9ER cancer cells after treatment with TKIs. Over four days, $TNF-\alpha$ mRNA levels increased when (A) H1975 cells were treated with 100 nM osimertinib, (B) HCC78 cells were treated with 1 μ M crizotinib, and (C) PC9ER cells were treated with 100 nM osimertinib. Plotted values are means (with standard deviations). mRNA = messenger ribonucleic acid; qPCR = quantitative polymerase chain reaction; TKI = tyrosine kinase inhibitor; $TNF-\alpha$ = tumor necrosis factor alpha.

Role of CD74 in Anti-Apoptosis

An assessment was made of the role of CD74 in anti-apoptosis mechanisms. First, H1975 cells were treated with 100 nM osimertinib for 48 hours to induce CD74 cells, which were sorted into CD74-positive and CD74-negative cells. These cells were then plated into 96-well plates and treated with 100 nM osimertinib, 1000 nM osimertinib, or no treatment, and a caspase assay was conducted. **Figure 5A** shows the flowchart of how CD74-positive and -negative cells were sorted. According to **Figure 5B**, CD74-positive cells that were induced by osimertinib treatment significantly inhibited apoptosis compared with CD74-negative cells. CD74-negative cells showed significantly higher relative luminescence values at both doses of osimertinib compared with CD74-positive cells. This data indicated that the presence of CD74 plays a role in inhibiting apoptosis.

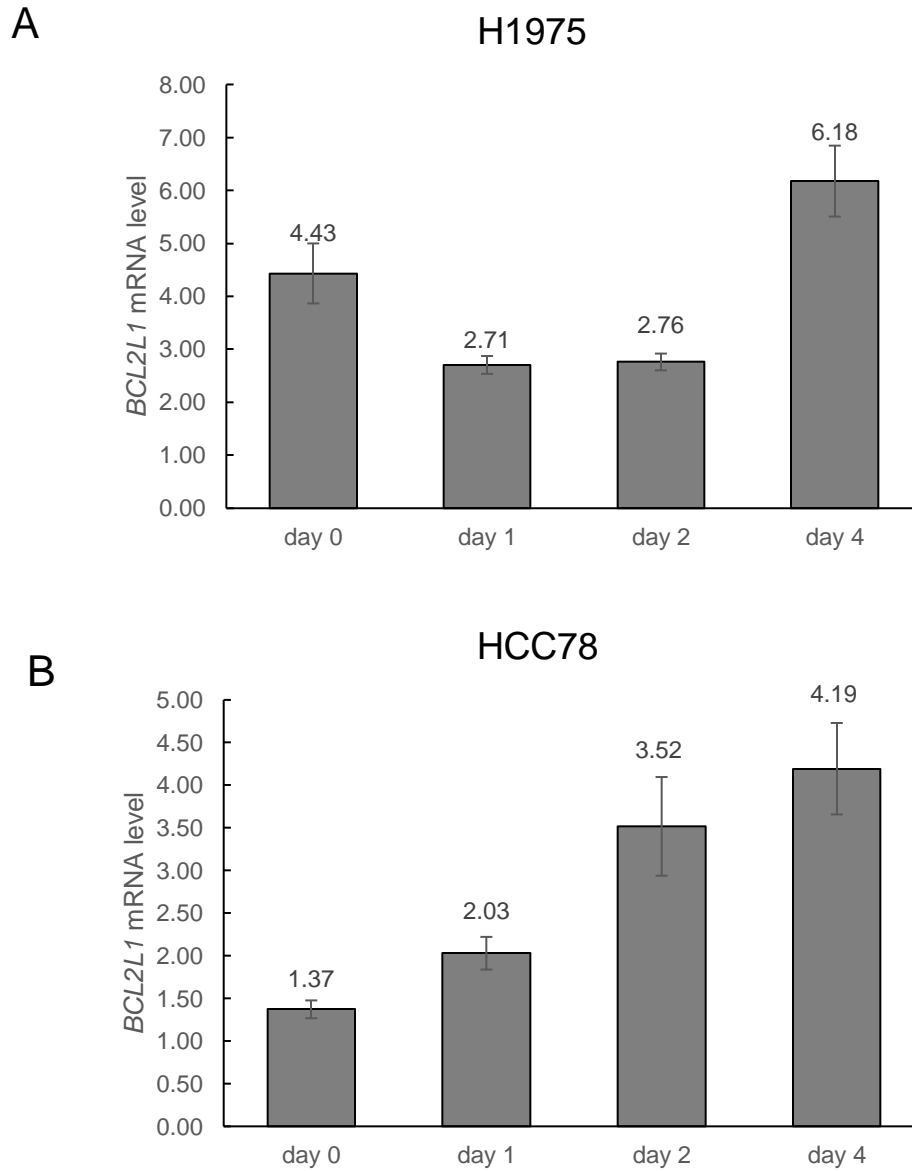
Figure 5*Caspase Assay in H1975 Cells Treated With Osimertinib*

Note. This figure shows the caspase assay procedure and results for H1975 cells treated with osimertinib. (A) A flowchart for the Caspase-Glo 3/7 assay (Promega) indicates that H1975 cells were treated with 100 nM osimertinib for 48 hours to induce CD74 cells, which were then sorted into CD74-positive and CD74-negative cells. (B) This plot compares caspase 3/7 activity (relative luminescence) for CD74-positive and CD74-negative cells that were untreated, treated with 100 nM osimertinib for 48 hours, or treated with 1000 nM osimertinib for 48 hours. Plotted values are means (with standard deviations). Caspase 3/7 = caspases-3 and -7; CD74 = cluster of differentiation 74; MIF = migration inhibitory factor. ** $p < .005$; ns = no significance.

CD74 also activates NF- κ B, which is a transcription factor inducing *BCL2L1* (De et al., 2018; Shostak & Chariot, 2015). *BCL2L1* is a gene that encodes for the protein BCL-XL that is involved in the inhibition of apoptosis and the promotion of cell survival (Loo et al., 2020). When the cytokine MIF binds to CD74, a cascade is initiated that leads

to NF- κ B activation and an increase in B-cell lymphoma-2 (Bcl-2) protein (Klasen et al., 2018).

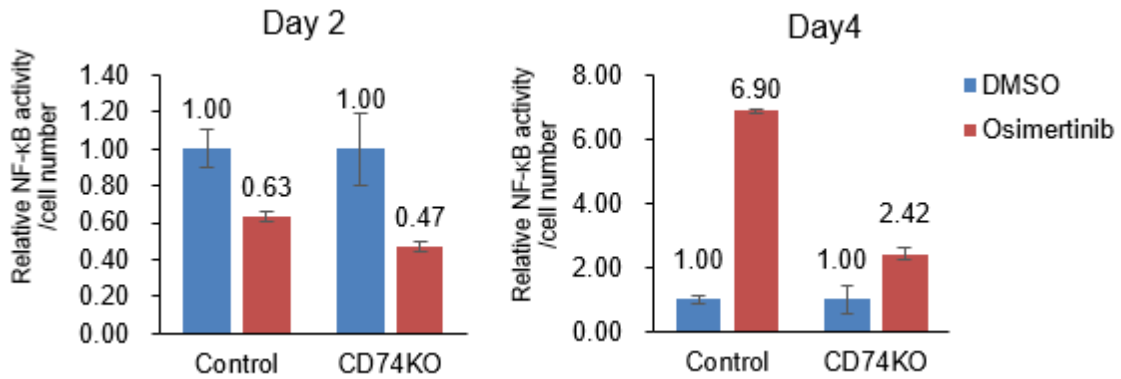
Experiments were carried out to assess the levels of *BCL2L1* in cancer cells after treatment with TKIs. H1975 cells were treated with 100 nM osimertinib and then measured for *BCL2L1* using qPCR. According to the results (**Figure 6A**), *BCL2L1* decreased after TKI administration but then increased by 96 hours, indicating an overall increase in *BCL2L1* mRNA levels by day 4 of treatment with osimertinib in H1975 cells. In HCC78 cells, *BCL2L1* mRNA levels also increased after TKI administration (**Figure 6B**). These results suggest that cancer cells being treated with TKIs are activating pathways which lead to suppression of apoptosis through BCL-XL mechanisms.

Figure 6*BCL2L1 mRNA Levels in H1975 and HCC78 Cancer Cells*

Note. This figure shows the qPCR results for *BCL2L1* mRNA levels in H1975 cells after treatment with TKIs. Over four days, *BCL2L1* mRNA levels increased when (A) H1975 cells were treated with 100 nM osimertinib, and (B) HCC78 cells treated with 1 μ M crizotinib. Plotted values are means (with standard deviations). *BCL2L1* = Bcl-2-like protein 1; mRNA = messenger ribonucleic acid; qPCR = qualitative polymerase chain reaction; TKI = tyrosine kinase inhibitor.

After *BCL2L1* mRNA levels were checked, the next step was to investigate the relationship between CD74 and NF- κ B. NF- κ B has been reported to be a transcription factor for *BCL2L1* (De et al., 2018). Because CD74 and *BCL2L1* expression levels were shown to increase after TKI treatment, a test was planned to determine if these levels were upregulated by NF- κ B. Testing was done with two different cell lines, Ctrl-NF- κ B-H1975 and CD74KO-NF- κ B-H1975. Both cell lines were treated with 30 nM osimertinib for 2 or 4 days, and then a reporter assay was conducted.

Figure 7 shows the results of this testing. On day 2 of the test, a decrease in NF- κ B activity was observed for both control and CD74KO cells treated with osimertinib compared with DMSO-treated samples. In particular, CD74KO cells were found to experience a greater reduction in NF- κ B activity than the control group. On day 4 of the test, osimertinib-treated samples had an increased NF- κ B activity compared with DMSO-treated samples. However, NF- κ B activity in control cells treated with osimertinib was higher than the CD74KO cells that were treated with osimertinib. Therefore, an increase in CD74 seems to promote anti-apoptosis by upregulating *BCL2L1* through NF- κ B.

Figure 7*NF-κB Activity in H1975 Cells*

Note. This figure shows NF-κB activity in H1975 control and knockout cells treated with 30 nM osimertinib (red) or DMSO (blue) on days 2 and 4 of the experiment. Plotted values are means (with standard deviations). CD74KO = cluster of differentiation 74 knockout; DMSO = dimethyl sulfoxide; NF-κB = nuclear factor kappa B.

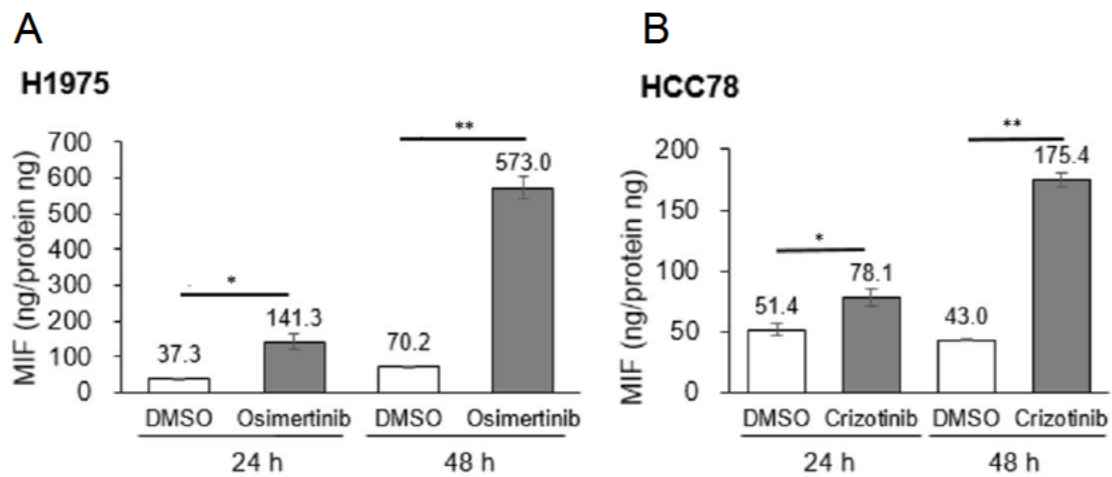
Targeting MIF

MIF is a pro-inflammatory cytokine that works to activate other inflammatory cytokines (like TNF- α and IFN- γ) and has been found in high numbers in almost all cancers (Nobre et al., 2017). MIF is a ligand for the receptor CD74 and seems to activate the AKT pathway, leading to activation of NF-κB and BCL-XL (Nobre et al., 2017). It has also been reported that MIF contributes to the tumor microenvironment by being secreted by tumor cells and macrophages through autocrine and paracrine secretion. To assess levels of MIF secretion from cancer cells after treatment with TKIs, ELISA was conducted with H1975 and HCC78 cells lines treated with 100 nm osimertinib and 2 μ M crizotinib, respectively. According to the results in **Figure 8**, MIF protein expression

levels significantly increased in both H1975 and HCC78 cells that were treated with TKIs by day 1 ($p < .05$), and even more so by day 2 ($p < .005$), compared with untreated samples. This confirms that MIF is secreted from tumor cells in an autocrine fashion after treatment with TKIs.

Figure 8

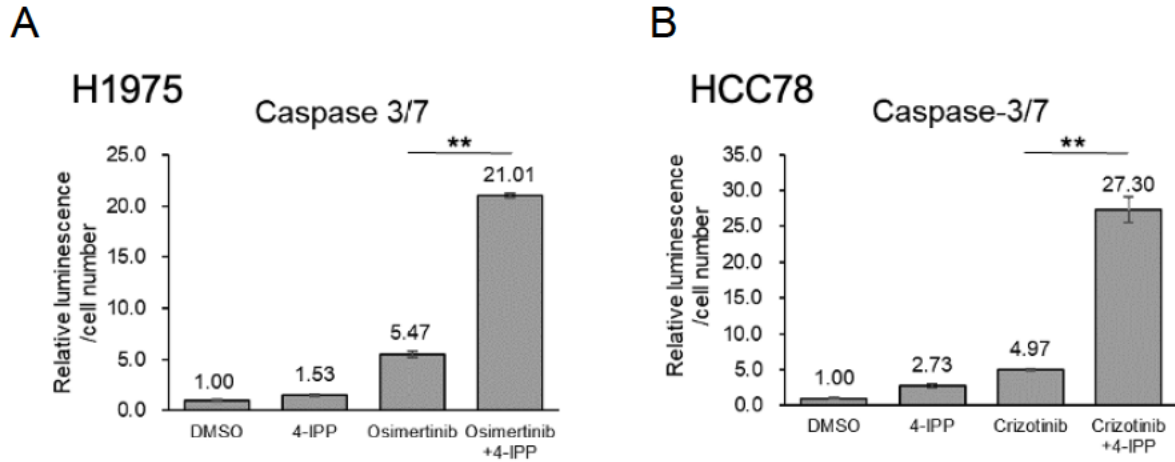
ELISA Results Measuring MIF of H1975 and HCC78 Cells



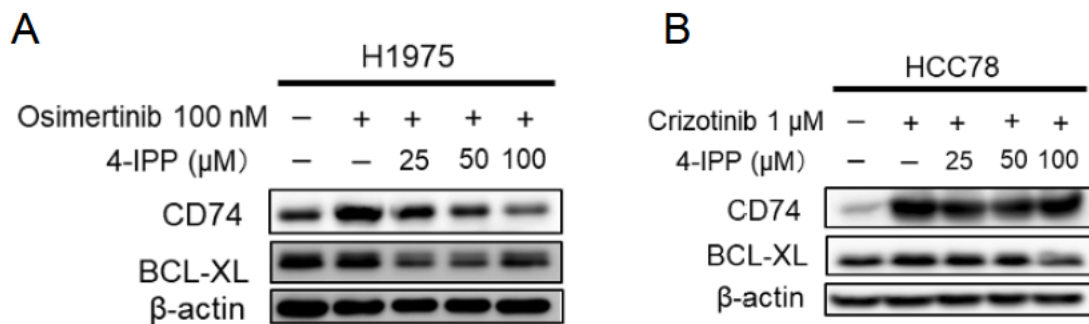
Note. This figure shows ELISA results measuring MIF of (A) H1975 cells treated with 100 nM osimertinib and (B) HCC78 cells treated with 2 μ M crizotinib. Plotted values are means (with standard deviations). DMSO = dimethyl sulfoxide; ELISA = enzyme-linked immunosorbent assay; MIF = migration inhibitory factor. * $p < 0.05$; ** $p < .005$.

The synergistic effects of MIF inhibitors and TKIs were tested by treating H1975 and HCC78 cells with TKIs, 100 nM osimertinib and 1 μ M crizotinib, respectively, in combination with or without an MIF inhibitor, 4-iodo-6-phenylpyrimidine (4-IPP). Based on the results from caspase 3/7 assays, western blotting, and qPCR, combination therapy

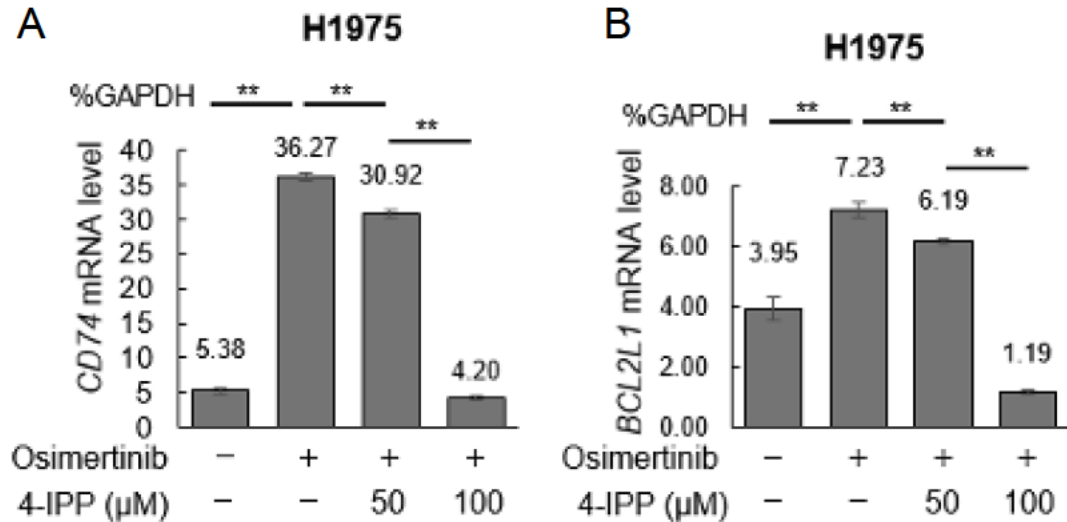
of TKIs with 4-IPP showed increased apoptosis and the greatest reduction of CD74 and BCL-XL and *BCL2L1* expression levels. In **Figure 9**, the combination therapy of osimertinib and 4-IPP or crizotinib and 4-IPP significantly increased caspase activity compared with TKI alone in both cell lines ($p < .005$). The results from western blots in **Figure 10** indicated that CD74 and BCL-XL expressions decreased with increasing MIF inhibitor dosage in H1975. However, in HCC78, BCL-XL expression decreased with increasing MIF inhibitor concentration, but CD74 expression showed no decrease. In **Figure 11**, the results from qPCR, in which *CD74* mRNA and *BCL2L1* mRNA levels were measured, showed that when H1975 cells were treated with a TKI, there was a significant increase in both *CD74* and *BCL2L1* mRNA levels ($p < .005$). When these cells were also treated with an MIF inhibitor at two concentrations (50 and 100 μM), *CD74* and *BCL2L1* mRNA levels significantly dropped from the high of TKI alone, especially with the higher dose of MIF inhibitor ($p < .005$). These data suggest that the combination of TKIs and MIF inhibitors has synergistic effects leading to greater antitumor effects.

Figure 9*Caspase Activity of H1975/HCC78 Treated With TKIs and MIF Inhibitor*

Note. This figure shows caspase 3/7 activity of (A) H1975 cells treated with 100 nM osimertinib with or without 4-IPP (MIF inhibitor) and (B) HCC78 cancer cells treated with 1 μ M crizotinib with or without 4-IPP. Plotted values are means (with standard deviations). 4-IPP = 4-iodo-6-phenylpyrimidine; DMSO = dimethyl sulfoxide. ** $p < .005$.

Figure 10*Western Blot Results of H1975/HCC78 Treated With TKIs and MIF Inhibitor*

Note. This figure shows western blotting results measuring CD74 and BCL-XL in (A) H1975 cells treated with 100 nM osimertinib with or without 4-IPP (MIF inhibitor) and (B) HCC78 cells treated with 1 μ M crizotinib with or without MIF inhibitor. Plotted values are means (with standard deviations). β -actin = control for western blots; 4-IPP = 4-iodo-6-phenylpyrimidine; CD74 = cluster of differentiation 74; BCL-XL = B-cell lymphoma-extra large.

Figure 11*CD74 and BCL2L1 mRNA Levels in H1975 Treated With TKI and MIF Inhibitor*

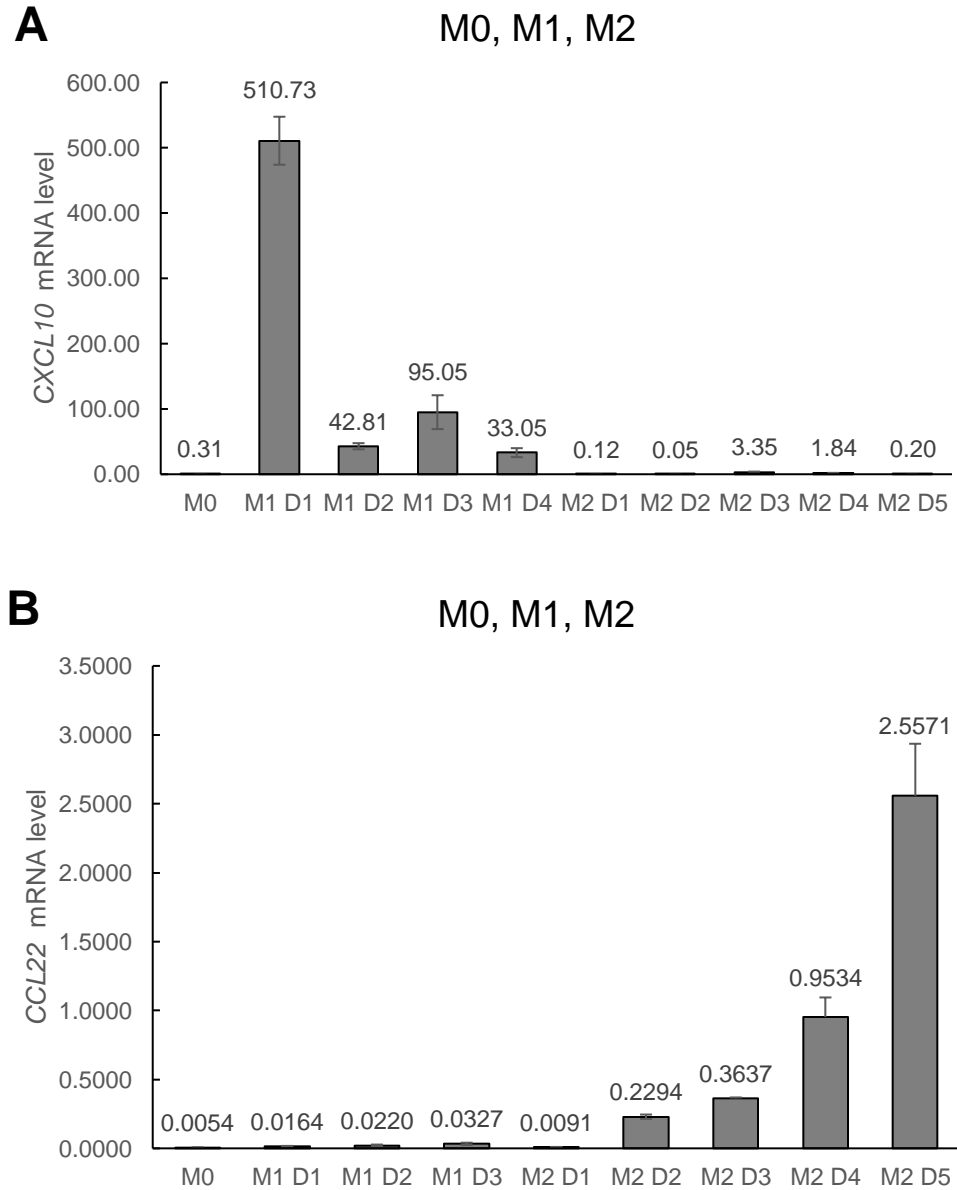
Note. This figure shows the qPCR results measuring (A) *CD74* and (B) *BCL2L1* mRNA expression levels in H1975 cells treated with 100 nM osimertinib with or without 4-IPP (MIF inhibitor). Plotted values are means (with standard deviation). 4-IPP = 4-iodo-6-phenylpyrimidine; BCL2L1 = Bcl-2-like protein 1; CD74 = cluster of differentiation 74; MIF = migration inhibitory factor; mRNA = messenger ribonucleic acid; qPCR = qualitative polymerase chain reaction; TKI = tyrosine kinase inhibitor.

Co-Culturing Macrophages With Cancer Cells

The tumor microenvironment is important to investigate because it contains cells from the immune system like macrophages. Macrophages have two main polarizations, M1 and M2. M1 macrophages are known to work in pro-inflammatory mechanisms and play a role in killing tumor cells. They release cytokines that inhibit the proliferation of surrounding cells, have high antigen presentation, and produce large amounts of nitric oxide and reactive oxygen intermediates (Wang et al., 2014). On the other hand, M2

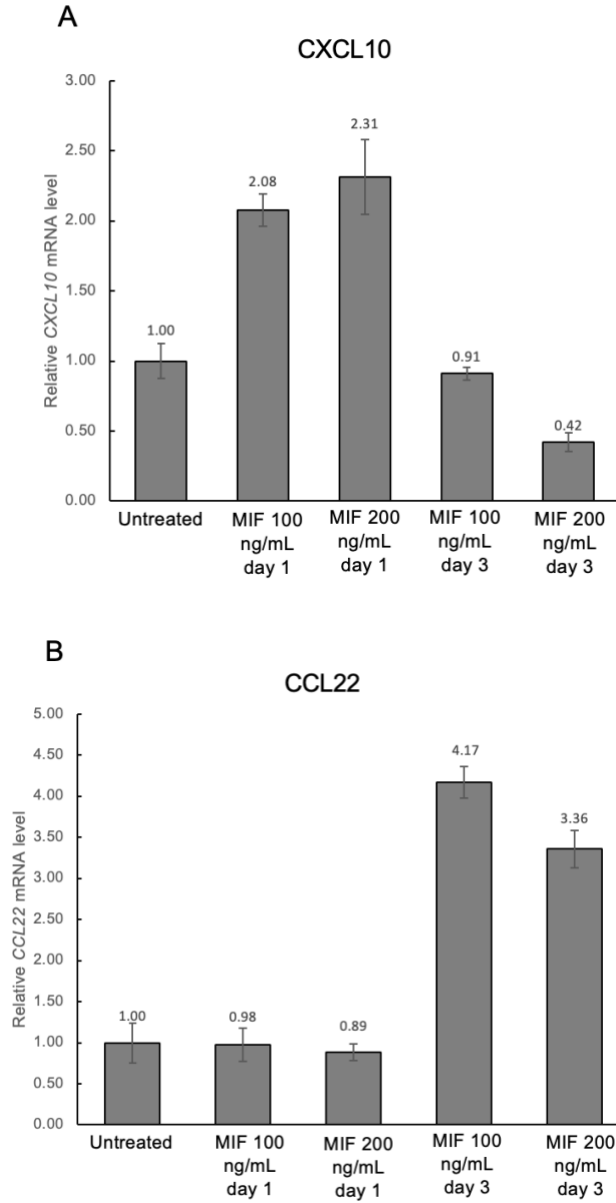
macrophages secrete anti-inflammatory cytokines that aid tumor development and are therefore considered pro-tumorigenic (Chen et al., 2019). Macrophages are unique in that they are plastic cells, and as such, they can be repolarized into M0, M1, and M2 macrophages depending on the conditions.

Experiments were undertaken to induce M0 macrophages to M1 macrophages by incubation with lipopolysaccharide (LPS) and IFN- γ and to M2 macrophages by incubation with IL-4 and IL-13. From qPCR results, the *CXCL10* mRNA level was the most sensitive marker of M1, which peaked on day 1 (**Figure 12A**), and the *CCL22* mRNA level was the most sensitive marker of M2, which increased by day 3 (**Figure 12B**).

Figure 12*CXCL10 and CCL22 mRNA Levels in M0, M1, and M2 Macrophages*

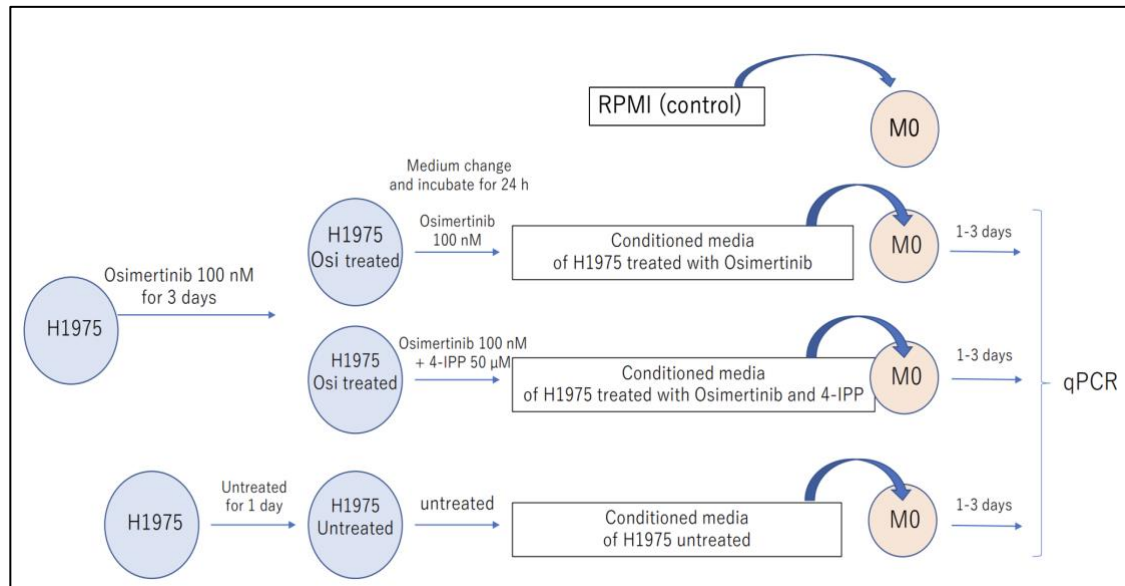
Note. This figure shows qPCR results showing (A) *CXCL10* mRNA levels and (B) *CCL22* mRNA levels in M0, M1, and M2 macrophages. Plotted values are means (with standard deviation). *CCL22* = chemokine ligand 22; *CXCL10* = C-X-C motif chemokine 10; mRNA = messenger ribonucleic acid; qPCR = qualitative polymerase chain reaction.

Because MIF is secreted from tumor cells, the next experiments were carried out to examine the effect of MIF on macrophage polarization. M0 macrophages were treated with recombinant MIF (100 ng/mL or 200 ng/mL), and qPCR was subsequently conducted to measure *CXCL10*, an M1 marker, and *CCL22*, an M2 marker (**Figure 13**). From qPCR results, *CXCL10* mRNA levels were higher than untreated M0 macrophages on day 1 but decreased by day 3 for both concentrations (**Figure 13A**). However, *CCL22* mRNA levels increased by day 3 on treatment with MIF compared with untreated M0 macrophages (**Figure 13B**). These results suggest that treatment with MIF induced M2 macrophages as seen with increased *CCL22* mRNA levels by day 3.

Figure 13*CXCL10 and CCL22 mRNA Levels in M0 Macrophages Treated With MIF*

Note. This figure shows qPCR results of (A) *CXCL10* mRNA levels and (B) *CCL22* mRNA levels in M0 macrophages treated with 100 ng/mL or 200 ng/mL MIF. Plotted values are means (with standard deviation). CCL22 = chemokine ligand 22; CXCL10 = C-X-C motif chemokine 10; mRNA = messenger ribonucleic acid; qPCR = qualitative polymerase chain reaction.

For a better understanding of the interaction between macrophages and cancer cells, M0 macrophages were cultured with CM from cancer cells (see **Figure 14**). The collection of CM was initiated by first seeding H1975 and treating the cells for 3 days with 100 nM osimertinib. After 3 days, one dish was treated again with 100 nM osimertinib, and another dish was treated with 100 nM osimertinib and 50 μ M 4-IPP. After 24 hours, the CM was collected from all dishes and then co-cultured with M0 macrophages. Controls for the experiment consisted of CM from untreated H1975 cells and from M0 macrophages cultured with RMPI. The dishes were incubated for an additional 24–72 hours, followed by qPCR experiments measuring M1 and M2 markers such as CXCL10 and CCL22, respectively.

Figure 14*Collecting Conditioned Media From Cancer Cells and Co-Culturing With Macrophages*

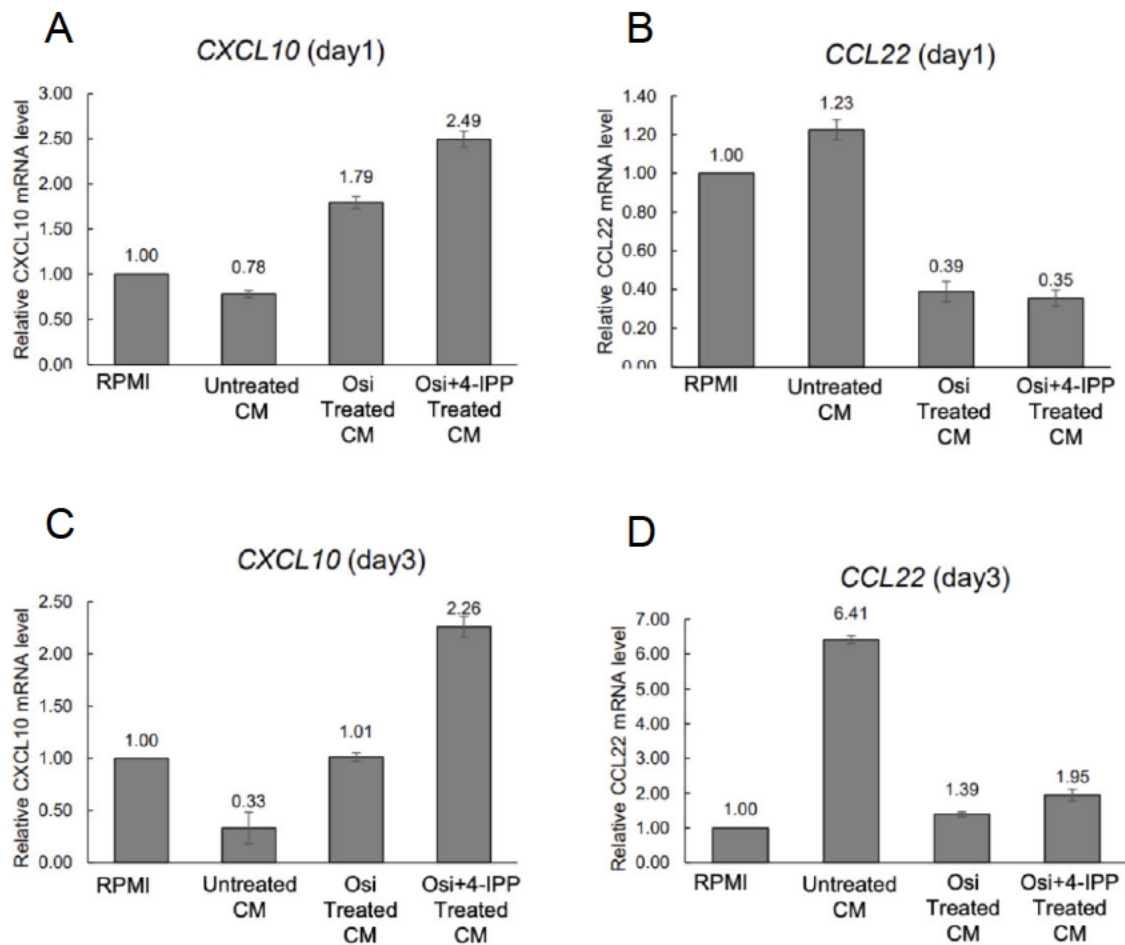
Note. This figure outlines the procedure for collecting conditioned medium from cancer cells and co-culturing with M0 macrophages. 4-IPP = 4-iodo-6-phenylpyrimidine; M0 = M0 macrophages; Osi = osimertinib; qPCR = quantitative polymerase chain reaction; RPMI = Roswell Park Memorial Institute medium

The qPCR results for these experiments are shown in **Figure 15**. The CM from H1975 cells treated with 100 nM osimertinib induced M1 macrophages as indicated by elevated CXCL10 expression on days 1 and 3 of treatment (**Figure 15A,C**). When H1975 cells were treated with 100 nM osimertinib and 50 μM 4-IPP combination therapy, this further promoted M1 induction (**Figure 15A,C**). For M2 macrophages, the qPCR results showed that *CCL22* (M2 marker) mRNA levels peaked in macrophages co-cultured in CM from untreated H1975 cells (**Figure 15B,D**). This suggests that CM from untreated

H1975 cells induced M2 macrophage expression compared with CM from treated H1975 cells.

Figure 15

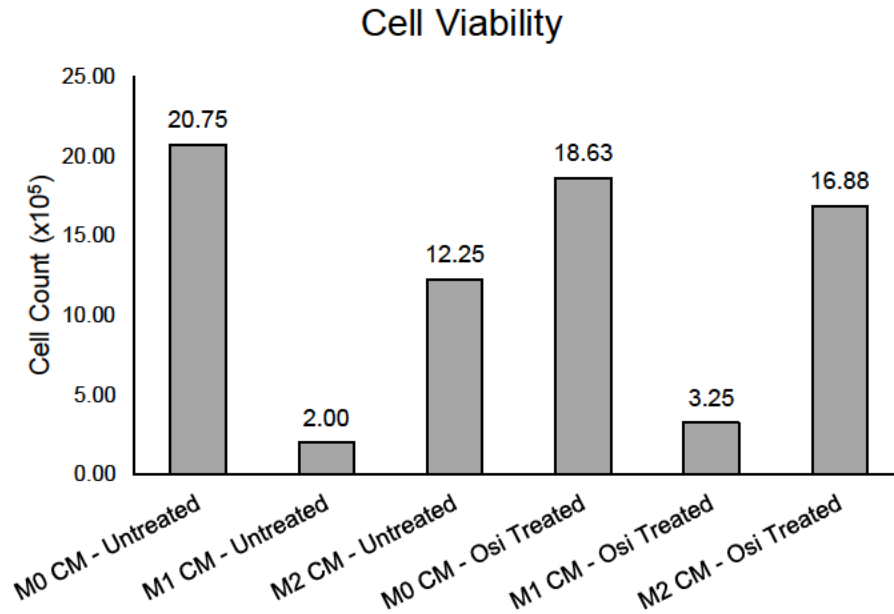
CXCL10 and CCL22 mRNA levels in H1975 Treated With TKIs and 4-IPP



Note. This figure shows qPCR results of (A,C) *CXCL10* (M1 marker) mRNA levels and (B,D) *CCL22* (M2 marker) mRNA levels in M0 macrophages that were co-cultured with conditioned media from H1975 cells with or without TKI and 4-IPP treatment on days one and three of treatment. Plotted values are means (with standard deviation). 4-IPP = 4-iodo-6-phenylpyrimidine; CCL22 = chemokine ligand 22; CM = conditioned medium; CXCL10 = C-X-C motif chemokine 10; mRNA = messenger ribonucleic acid; osi = osimertinib; qPCR = qualitative polymerase chain reaction.

Next, experiments were done to investigate the effect of macrophages on tumors. After macrophages were induced to M0, M1, and M2 polarization, the CM was collected and then incubated with H1975 cancer cells for one to three days. H1975 cells were cultured in M0 CM, M1 CM, or M2 CM, and at each condition, the cells were either treated with osimertinib or left untreated.

These cells were then collected and counted to assess cell viability (**Figure 16**). The cell counts for H1975 cells were highest in untreated cells that were cultured in RPMI. The lowest cell counts were for cells that were cultured in M1 CM in both untreated and osimertinib-treated conditions. These results suggest that cytokines and chemokines from M1 macrophages may have antitumor effects as seen with the reduced cell counts.

Figure 16*Cell Viability in H1975 Cells in Macrophage Conditioned Media*

Note. This figure shows cell viability in H1975 cells cultured with M0, M1, or M2 conditioned media and were either left untreated or were treated with osimertinib. Plotted values are means. M0 CM = M0 macrophage-conditioned media; M1 CM = M1 macrophage-conditioned media; M2 CM = M2 macrophage-conditioned media; osi = osimertinib.

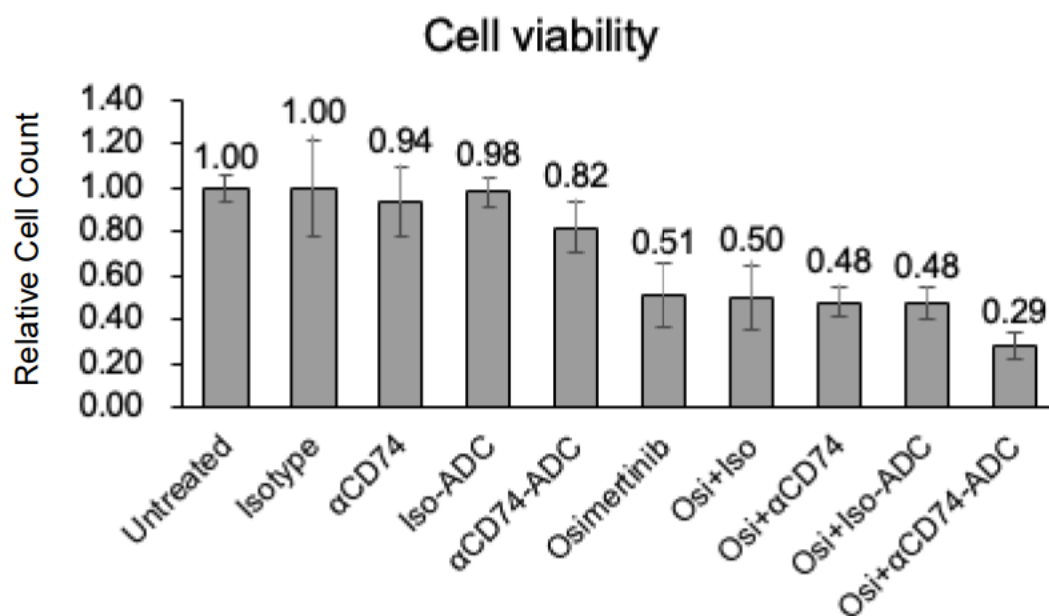
Targeting CD74 with Anti-CD74-ADC

This study also focused on CD74 as a new therapeutic target, especially because anti-CD74 antibodies are possible (candidate) treatments for lymphoma and myeloma. Antibody-drug conjugates (ADCs) are monoclonal antibodies that are chemically linked to a cytotoxic payload. The antibody binds to specific proteins or receptors on target cells and allows the linked drug to enter the cell. This method increases tumor specificity and limits systematic exposure which increases tolerability and safety.

For this study, anti-CD74-ADC was generated consisting of milatuzumab as the antibody, MMAE as the drug, and VC-PAB as the linker. Experiments were initiated to test the efficacy of these anti-CD74-ADCs. To start, H1975 cells were seeded into a 96-well plate (2,000 cells/well) and were maintained in either an untreated condition or an osimertinib (30 nM)-treated condition with or without anti-CD74-ADC (25 $\mu\text{g}/\text{mL}$). Cell viability was then determined as shown in **Figure 17**. Combination therapy of osimertinib and anti-CD74-ADC significantly decreased cell numbers compared with the combination of osimertinib and iso-ADC.

Figure 17

Cell Viability in H1975 Cells Treated With Osimertinib and Antibody



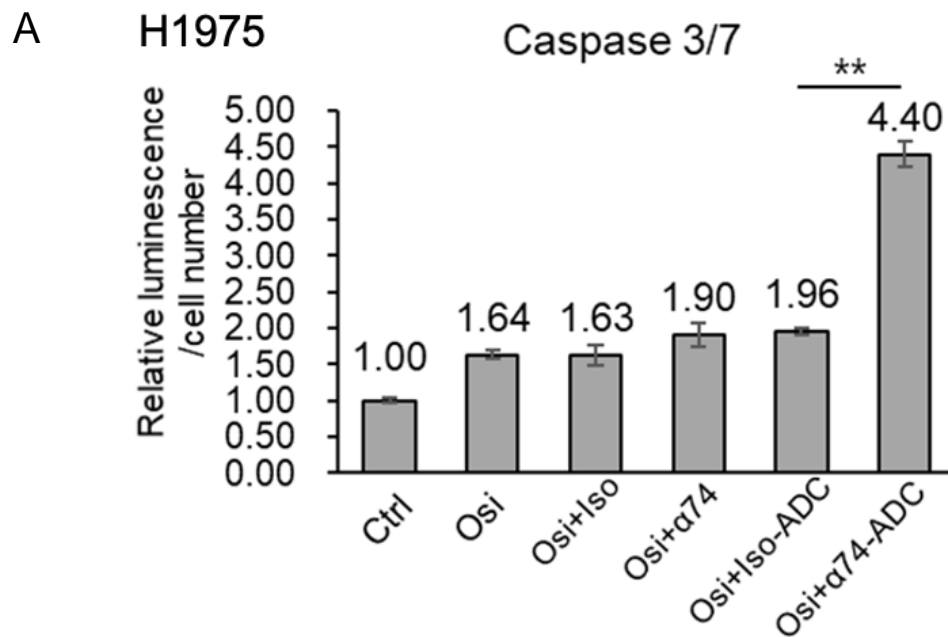
Note. This figure shows cell viability in H1975 cells treated with 30 nM osimertinib with or without 25 µg/mL antibody. Plotted values are means (with standard deviations). αCD74 = anti-CD74; ADC = antibody-drug conjugate; CD74 = cluster of differentiation 74; Iso = isotype; Osi = osimertinib.

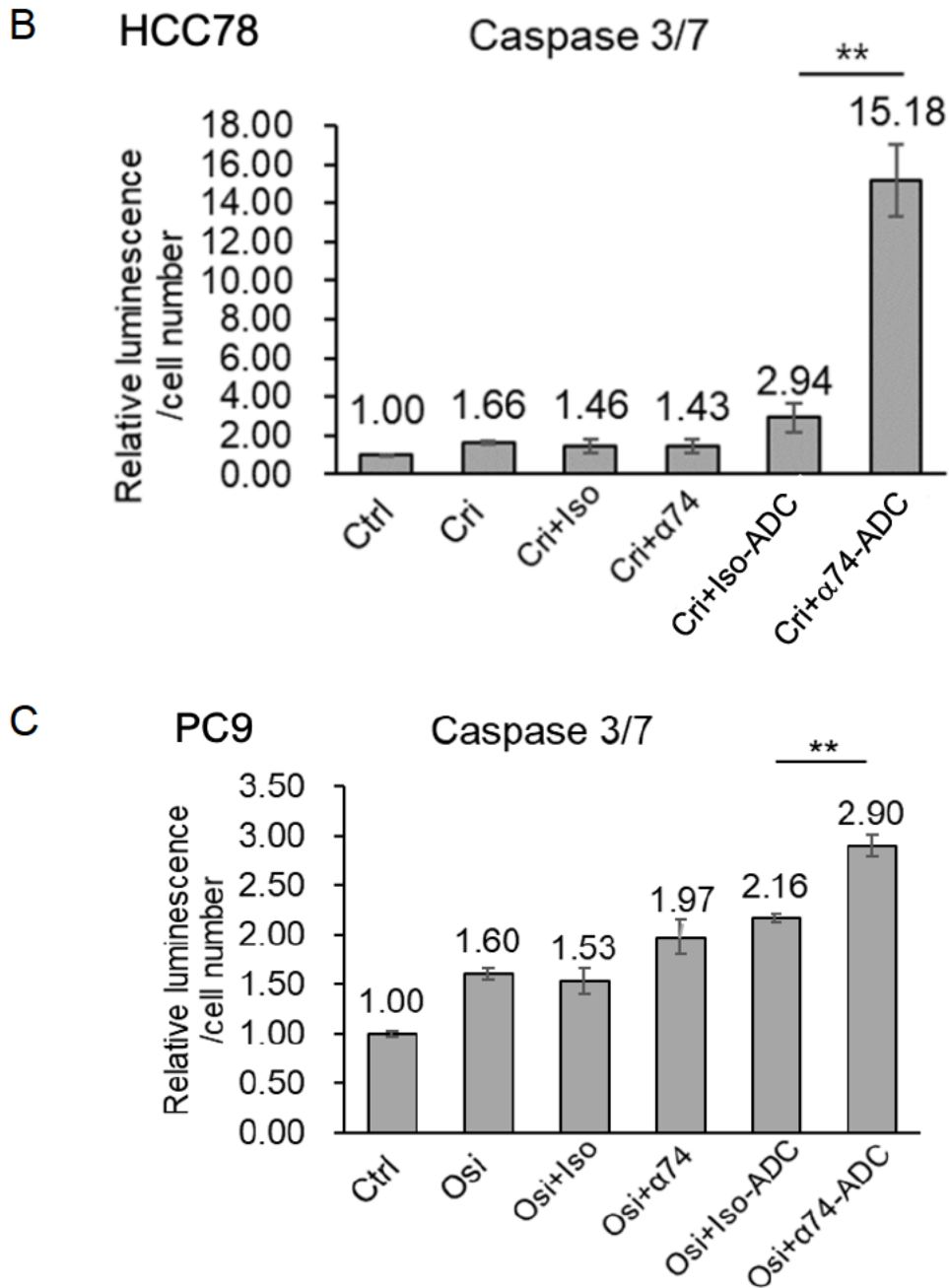
Apoptosis assays were conducted in H1975, HCC78, and PC9 cancer cells treated with TKIs with or without the anti-CD74-ADCs. H1975 and HCC78 showed high expression of CD74 compared with PC9 in previous experiments (**Figure 2**). Anti-CD74-ADC alone also somewhat increased caspase activity in all cell lines. Although caspase activity was slightly elevated in conditions where the TKI or the anti-CD74-ADC was the sole treatment in all cell lines, the caspase activity was significantly greater in conditions where TKIs were in combination therapy with the anti-CD74-ADC. The results in **Figure**

18 indicated that for all cell lines, the combination therapy of osimertinib and anti-CD74-ADC showed a significantly higher caspase activity, indicating more apoptosis occurring in this condition ($p < .005$). All cell lines also showed significant difference in caspase activity between (TKIs + anti-CD74) and (TKIs + iso-ADC), suggesting that combining TKIs with ADCs could deliver a more robust antitumor effect.

Figure 18

Apoptosis Assays in H1975, HCC78, and PC9 With TKIs and Antibody

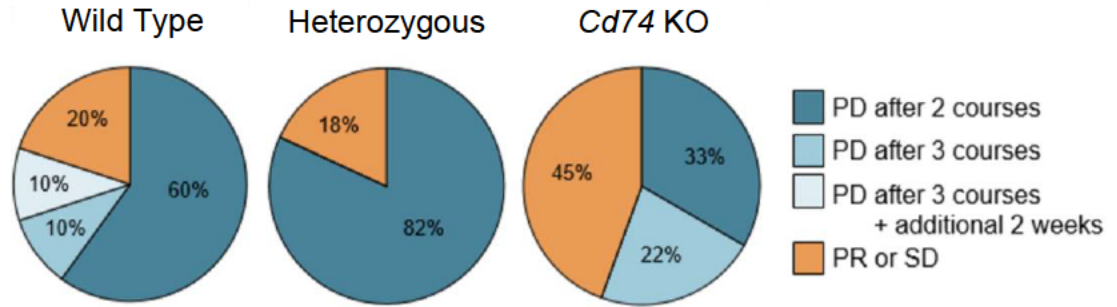




Note. This figure shows the results of apoptosis assays measuring caspase activity (caspase 3/7) in (A) H1975, (B) HCC78, and (C) PC9 cells. H1975 and PC9 were treated with osimertinib with or without anti-CD74-ADCs. HCC78 was treated with crizotinib with or without anti-CD74-ADCs. Plotted values are means (with standard deviations). α74 = anti-CD74; ADC = antibody-drug conjugate; Cri = crizotinib; Iso = isotype, Ctrl = control; Osi = osimertinib; TKI = tyrosine kinase inhibitor. $**p < .005$.

Complete Deletion of CD74 Suppresses TKI Resistance *In Vivo*

In vivo models were conducted in doxycycline-inducible, EGFR-mutated, lung-specific cancer mouse models. The results are summarized in the pie charts of **Figure 19**. In wild type (WT) mice (left pie chart), 20% showed a partial response (PR) or stable disease (SD), and the rest experienced disease progression (PD) after 2–3 courses of treatment. The middle pie chart signifies a heterozygous model of WT and KO. In this group, 18% exhibited PR or SD, and the remainder showed disease progression after two courses of treatment. However, CD74 KO (**Figure 19**) mice (right pie chart) showed a robust response of 45% PR or SD as well as a delayed resistance reflected by a decreased percentage for the “PD after 2 courses.” Overall, these results indicated that a complete deletion of CD74 overcame or delayed resistance to TKIs.

Figure 19*CD74 Knockout Suppresses Resistance to EGFR-TKIs In Vivo*

Note. This figure shows the doxycycline-inducible, EGFR-mutated, lung-specific cancer mouse model with wild type, heterozygous, and *Cd74* KO mice treated with osimertinib. CD74 = cluster of differentiation 74; EGFR = epithelial growth factor receptor; KO = knockout; PD = progressive disease; PR = partial response; SD = stable disease; TKI = tyrosine kinase inhibitor.

DISCUSSION

Intrinsic or acquired drug resistance poses a difficult challenge in the treatment of lung cancers. There are multiple mechanisms of resistance, such as activation of alternative signaling, acquisition of a secondary mutation (e.g., T790M), or impairment of apoptosis pathways (Morgillo et al., 2016). Targeting DTP cells has been highlighted as an effective approach to combat resistance to TKIs in oncogene-mutated NSCLCs. This study demonstrated that the MIF-CD74 axis plays an important role in the formation of DTP cells and that this axis might be a novel target for overcoming resistance to TKIs.

Although various DTP cell markers have been identified, the definition of DTP cells is immature. So far, there are two defining features of DTP cells. The first characteristic is that DTP cells are alive but not fully proliferative or resistant during drug treatment because of a slow cell cycle and evasion of drug-induced apoptosis. Second, their drug-tolerant state is reversible upon removal of the drug. In the DTP model of this study, TKIs were administered at concentrations sufficiently higher than the half-maximal inhibitory concentration (IC_{50}). Under this condition, cell proliferation stopped, and the cell cycle slowed, but proliferation resumed after removal of TKIs. Previous papers have identified various DTP cell markers such as kinase receptor genes (e.g., AXL, FGFR3, IGF-1R) and pathways involved in transcriptional activation (e.g. Wnt/ β -catenin, Aurora kinase, YAP-TEAD) (Arasada et al., 2018; Kurppa et al., 2020; Raouf et al., 2019; Shah et al., 2019; Taniguchi et al., 2019; Wang et al., 2020). It has also been reported that CD74 can be a potential DTP cell marker (Kashima et al., 2021). However,

elucidating the mechanisms of DTP cell formation and developing effective therapies remain unknown.

In this study, CD74 expression was demonstrated to be related to CIITA upregulation through TKIs and treatment with TNF- α and IFN- γ in lung cancer. CIITA, upstream of CD74, is inhibited by EGFR signaling and is thereby upregulated when treated with TKIs. IFN- γ and TNF- α induce CD74 expression in melanoma and multiple myeloma, respectively (Klasen et al., 2018; Tanese et al., 2015). It has also been reported that TNF- α is upregulated after treatment with TKIs in EGFR-mutated lung cancers (Gong et al., 2018). This study found that tumor cells secrete TNF- α by autocrine signaling and induce CD74 expression to form DTP cells. IFN- γ also induced CD74 expression in lung cancer cell lines as well as cancers in other organ systems. However, IFN- γ does not seem to be released from tumors by autocrine secretion as no results were detected from qPCR and ELISA. These results showed the relationship between CD74 upregulation to CIITA, TNF- α , and IFN- γ in lung cancer. Furthermore, CD74 expression was found to suppress apoptosis through activating BCL-XL pathways.

In addition to genetic and epigenetic alterations within tumor cells, the interplay between tumor cells and their microenvironment can also play a role in the development of tumors and drug resistance. The TME is a complex network of cells and tissues that surrounds and supports the growth and survival of cancer cells within a tumor (Baghban et al., 2020). Tumor-associated macrophages are a significant part of the TME in various solid tumor types (Chen et al., 2019). Because macrophages and tumor cells both secrete

MIF, a ligand for CD74, further investigations in the interaction between the TME and tumor cells are needed.

Alveolar macrophages play an important role in antigen presentation in normal lungs. Macrophages have two main polarizations, M1 and M2. In oncology, M1 operates in a pro-inflammatory manner and induces apoptosis, whereas M2 works in a pro-tumoral environment. Macrophages have unique characteristics in that they can repolarize between M0, M1, and M2; thus, the tumor and tumor microenvironment can change the role of macrophages. Throughout the course of treatment with TKIs, the tumor microenvironment undergoes changes that have been described as drug-sensitive and drug-resistant periods (Jiang & Liu, 2022). The drug-sensitive period is characterized by an inflammatory microenvironment with decreased M2 macrophages and an increase in cytotoxic immune cells. TKIs initially induce expression of MHC class I and class II molecules to promote T cell-mediated tumor death, modulating immune-mediated cytotoxicity in the tumor microenvironment in this initial response period (Jiang & Liu, 2022). However, the drug-resistant period shows an increase in M2 macrophages, immunosuppressive cells, and the expression of immune checkpoint proteins. When resistance emerges after long-term use of TKIs, there is a reversal of positive therapeutic response and a notable decrease in cytotoxic T cell populations. In this study, when M1 CM and M2 CM were co-cultured with cancer cells, M1 CM induced apoptosis of tumor cells compared with M2 CM. When cancer cell CM was collected and co-cultured with M0 macrophages, untreated cancer cell CM induced M2 macrophages, whereas CM from cancer cells treated with TKIs induced M1 macrophages.

MIF has been noted for its pleiotropic behavior in that it can induce pro-inflammatory immune responses in the tumor microenvironment. However, in advanced diseases, it can also play a role in immune escape (Thiele et al., 2022). According to current literature, recombinant MIF (100 ng/mL) can induce M2 polarization in THP-1 cells (Thiele et al., 2022). It has also been reported that in metastatic melanoma models, macrophages can display M2 macrophage characteristics and exhibit a high expression of MIF (Gutiérrez-González et al., 2016).

In this study, macrophages and their interactions with tumor cells were investigated because macrophages can secrete MIF and TNF- α . *TNF- α* mRNA levels were higher in M1 macrophages than in M0 and M2 macrophages, and CM, containing TNF- α secreted from M1 macrophages, slightly induced CD74 upregulation in cancer cells. Because MIF normally induces M2 macrophages, MIF inhibitors contributed to M1 polarization. MIF inhibitors induced apoptosis of tumor cells and altered the immune environment in favor of antitumor effects. However, high drug concentrations were required to achieve the desired effect, making it difficult to use these inhibitors in *in vivo* experiments. Therefore, this study focused on targeting CD74. CD74 is known to rapidly internalize upon antibody engagement and traffic to the lysosome and to rapidly repopulate on the surface of tumor cells following internalization. Antibodies and antibody drug conjugates targeting CD74 have been shown previously to demonstrate antitumor activity in preclinical models of cancer (Li et al., 2023). In lung cancer cell lines, combination of TKIs and anti-CD74-ADCs showed significant synergistic effects, especially in cell lines that had high CD74 expression. Because CD74-expressing

macrophages also act in a pro-tumor manner before treatment with tumor microenvironment and at relapse, the reduction of macrophages by anti-CD74-ADCs might provide an advantage in antitumor efficacy.

The verification that CD74 can be a therapeutic target *in vivo* was demonstrated by crossing lung-specific *EGFR-L858R-T790M* transgenic mice with *Cd74* KO mice. *Cd74* KO mice also exhibit a significant reduction of thymic and peripheral CD4+ T cells and display a distinct defect of B cell maturation and function (Bikoff et al., 1993). However, complete deletion of CD74 did not affect mouse growth and survival. Based on the *in vivo* experiments of this study, *Cd74* KO mice showed that deletion of CD74 overcame or delayed disease progression.

Through these experiments, CD74 upregulation after treatment with TKIs was shown to be common in lung cancers with EGFR mutations and ROS1 fusions. Therapies targeting CD74 were effective in two different lung cancer mutations, and further work with this approach might lead to novel and much-needed therapies for lung cancer.

BIBLIOGRAPHY

- Abrahams, C. L., Li, X., Embry, M., Yu, A., Krimm, S., Krueger, S., . . . Molina, A. (2018). Targeting CD74 in multiple myeloma with the novel, site-specific antibody-drug conjugate STRO-001. *Oncotarget*, 9(102), 37700-37714.
<https://doi.org/10.18632/oncotarget.26491>
- American Lung Association. (2022, November 17). *Types of lung cancer*.
<https://www.lung.org/lung-health-diseases/lung-disease-lookup/lung-cancer/basics/lung-cancer-types#:~:text=There%20are%20two%20main%20types,lung%20cancer%20is%20called%20carcinoid>
- Arasada, R. R., Shilo, K., Yamada, T., Zhang, J., Yano, S., Ghanem, R., . . . Carbone, D. P. (2018). Notch3-dependent β -catenin signaling mediates EGFR TKI drug persistence in EGFR mutant NSCLC. *Nature Communications*, 9(1), 3198.
<https://doi.org/10.1038/s41467-018-05626-2>
- Baghban, R., Roshangar, L., Jahanban-Esfahlan, R., Seidi, K., Ebrahimi-Kalan, A., Jaymand, M., . . . Zare, P. (2020). Tumor microenvironment complexity and therapeutic implications at a glance. *Cell Communication and Signaling*, 18(1), 59. <https://doi.org/10.1186/s12964-020-0530-4>
- Bikoff, E. K., Huang, L. Y., Episkopou, V., van Meerwijk, J., Germain, R. N., & Robertson, E. J. (1993). Defective major histocompatibility complex class II assembly, transport, peptide acquisition, and CD4⁺ T cell selection in mice

lacking invariant chain expression. *Journal of Experimental Medicine*, 177(6), 1699-1712. <https://doi.org/10.1084/jem.177.6.1699>

Bruchez, A., Sha, K., Johnson, J., Chen, L., Stefani, C., McConnell, H., . . . Lacy-Hulbert, A. (2020). MHC class II transactivator CIITA induces cell resistance to Ebola virus and SARS-like coronaviruses. *Science*, 370(6513), 241-247. <https://doi.org/10.1126/science.abb3753>

Cancer Statistics Center. (n.d.). *Estimated new cases, 2023*. American Cancer Society. https://cancerstatisticscenter.cancer.org/?_ga=2.12676215.1561791906.1674412324-354082034.1670379623#!/

Chen, Y., Song, Y., Du, W., Gong, L., Chang, H., & Zou, Z. (2019). Tumor-associated macrophages: an accomplice in solid tumor progression. *Journal of Biomedical Science*, 26(1), 78. <https://doi.org/10.1186/s12929-019-0568-z>

De, R., Sarkar, S., Mazumder, S., Debsharma, S., Siddiqui, A. A., Saha, S. J., . . . Bandyopadhyay, U. (2018). Macrophage migration inhibitory factor regulates mitochondrial dynamics and cell growth of human cancer cell lines through CD74-NF- κ B signaling. *Journal of Biological Chemistry*, 293(51), 19740-19760. <https://doi.org/10.1074/jbc.RA118.003935>

Gazdar, A. F. (2009). Activating and resistance mutations of EGFR in non-small-cell lung cancer: role in clinical response to EGFR tyrosine kinase inhibitors. *Oncogene*, 28 Suppl 1(Suppl 1), S24-31. <https://doi.org/10.1038/onc.2009.198>

Gong, K., Guo, G., Gerber, D. E., Gao, B., Peyton, M., Huang, C., . . . Habib, A. A. (2018). TNF-driven adaptive response mediates resistance to EGFR inhibition in

lung cancer. *Journal of Clinical Investigation*, 128(6), 2500-2518.

<https://doi.org/10.1172/JCI96148>

Gutiérrez-González, A., Martínez-Moreno, M., Samaniego, R., Arellano-Sánchez, N., Salinas-Muñoz, L., Relloso, M., . . . Sánchez-Mateos, P. (2016). Evaluation of the potential therapeutic benefits of macrophage reprogramming in multiple myeloma. *Blood*, 128(18), 2241-2252. <https://doi.org/10.1182/blood-2016-01-695395>

Hata, A. N., Niederst, M. J., Archibald, H. L., Gomez-Caraballo, M., Siddiqui, F. M., Mulvey, H. E., . . . Engelman, J. A. (2016). Tumor cells can follow distinct evolutionary paths to become resistant to epidermal growth factor receptor inhibition. *Nature Medicine*, 22(3), 262-269. <https://doi.org/10.1038/nm.4040>

Holling, T. M., Schooten, E., & van Den Elsen, P. J. (2004). Function and regulation of MHC class II molecules in T-lymphocytes: of mice and men. *Human Immunology*, 65(4), 282-290. <https://doi.org/10.1016/j.humimm.2004.01.005>

Jiang, L., & Liu, J. (2022). Immunological effect of tyrosine kinase inhibitors on the tumor immune environment in non-small cell lung cancer. *Oncology Letters*, 23(5), 165. <https://doi.org/10.3892/ol.2022.13285>

Kashima, Y., Shibahara, D., Suzuki, A., Muto, K., Kobayashi, I. S., Plotnick, D., . . . Kobayashi, S. S. (2021). Single-Cell Analyses Reveal Diverse Mechanisms of Resistance to EGFR Tyrosine Kinase Inhibitors in Lung Cancer. *Cancer Research*, 81(18), 4835-4848. <https://doi.org/10.1158/0008-5472.CAN-20-2811>

- Klasen, C., Ziehm, T., Huber, M., Asare, Y., Kapurniotu, A., Shachar, I., . . . El Bounkari, O. (2018). LPS-mediated cell surface expression of CD74 promotes the proliferation of B cells in response to MIF. *Cell Signalling*, *46*, 32-42.
<https://doi.org/10.1016/j.cellsig.2018.02.010>
- Kobayashi, S., Boggon, T. J., Dayaram, T., Jänne, P. A., Kocher, O., Meyerson, M., . . . Halmos, B. (2005). EGFR mutation and resistance of non-small-cell lung cancer to gefitinib. *New England Journal of Medicine*, *352*(8), 786-792.
<https://doi.org/10.1056/NEJMoa044238>
- Kurppa, K. J., Liu, Y., To, C., Zhang, T., Fan, M., Vajdi, A., . . . Jänne, P. A. (2020). Treatment-Induced Tumor Dormancy through YAP-Mediated Transcriptional Reprogramming of the Apoptotic Pathway. *Cancer Cell*, *37*(1), 104-122.e112.
<https://doi.org/10.1016/j.ccell.2019.12.006>
- Li, D., Shimamura, T., Ji, H., Chen, L., Haringsma, H. J., McNamara, K., . . . Wong, K. K. (2007). Bronchial and peripheral murine lung carcinomas induced by T790M-L858R mutant EGFR respond to HKI-272 and rapamycin combination therapy. *Cancer Cell*, *12*(1), 81-93. <https://doi.org/10.1016/j.ccr.2007.06.005>
- Li, X., Abrahams, C., Yu, A., Embry, M., Henningsen, R., DeAlmeida, V., . . . Molina, A. (2023). Targeting CD74 in B-cell non-Hodgkin lymphoma with the antibody-drug conjugate STRO-001. *Oncotarget*, *14*, 1-13.
<https://doi.org/10.18632/oncotarget.28341>
- Lin, J. J., Choudhury, N. J., Yoda, S., Zhu, V. W., Johnson, T. W., Sakhtemani, R., . . . Gainor, J. F. (2021). Spectrum of Mechanisms of Resistance to Crizotinib and

Lorlatinib in. *Clin Cancer Research*, 27(10), 2899-2909.

<https://doi.org/10.1158/1078-0432.CCR-21-0032>

Loo, L. S. W., Soetedjo, A. A. P., Lau, H. H., Ng, N. H. J., Ghosh, S., Nguyen, L., . . .

Teo, A. K. K. (2020). BCL-xL/BCL2L1 is a critical anti-apoptotic protein that promotes the survival of differentiating pancreatic cells from human pluripotent

stem cells. *Cell Death & Disease*, 11(5), 378. <https://doi.org/10.1038/s41419-020-2589-7>

Mikubo, M., Inoue, Y., Liu, G., & Tsao, M. S. (2021). Mechanism of Drug Tolerant Persister Cancer Cells: The Landscape and Clinical Implication for Therapy.

Journal of Thoracic Oncology, 16(11), 1798-1809.

<https://doi.org/10.1016/j.jtho.2021.07.017>

Morgillo, F., Della Corte, C. M., Fasano, M., & Ciardiello, F. (2016). Mechanisms of resistance to EGFR-targeted drugs: lung cancer. *ESMO Open*, 1(3), e000060.

<https://doi.org/10.1136/esmoopen-2016-000060>

Nobre, C. C., de Araújo, J. M., Fernandes, T. A., Cobucci, R. N., Lanza, D. C., Andrade, V. S., & Fernandes, J. V. (2017). Macrophage Migration Inhibitory Factor (MIF):

Biological Activities and Relation with Cancer. *Pathology and Oncology*

Research, 23(2), 235-244. <https://doi.org/10.1007/s12253-016-0138-6>

Pan, Y., Deng, C., Qiu, Z., Cao, C., & Wu, F. (2021). The Resistance Mechanisms and Treatment Strategies for ALK-Rearranged Non-Small Cell Lung Cancer.

Frontiers in Oncology, 11, 713530. <https://doi.org/10.3389/fonc.2021.713530>

- Pollack, B. P., Sapkota, B., & Cartee, T. V. (2011). Epidermal growth factor receptor inhibition augments the expression of MHC class I and II genes. *Clinical Cancer Research*, 17(13), 4400-4413. <https://doi.org/10.1158/1078-0432.CCR-10-3283>
- Ramalingam, S. S., Yang, J. C., Lee, C. K., Kurata, T., Kim, D. W., John, T., . . . Jänne, P. A. (2018). Osimertinib As First-Line Treatment of EGFR Mutation-Positive Advanced Non-Small-Cell Lung Cancer. *Journal of Clinical Oncology*, 36(9), 841-849. <https://doi.org/10.1200/JCO.2017.74.7576>
- Ramirez, M., Rajaram, S., Steininger, R. J., Osipchuk, D., Roth, M. A., Morinishi, L. S., . . . Altschuler, S. J. (2016). Diverse drug-resistance mechanisms can emerge from drug-tolerant cancer persister cells. *Nature Communications*, 7, 10690. <https://doi.org/10.1038/ncomms10690>
- Raouf, S., Mulford, I. J., Frisco-Cabanos, H., Nangia, V., Timonina, D., Labrot, E., . . . Hata, A. N. (2019). Targeting FGFR overcomes EMT-mediated resistance in EGFR mutant non-small cell lung cancer. *Oncogene*, 38(37), 6399-6413. <https://doi.org/10.1038/s41388-019-0887-2>
- Ruvolo, P. P., Hu, C. W., Qiu, Y., Ruvolo, V. R., Go, R. L., Hubner, S. E., . . . Kornblau, S. M. (2019). LGALS3 is connected to CD74 in a previously unknown protein network that is associated with poor survival in patients with AML. *EBioMedicine*, 44, 126-137. <https://doi.org/10.1016/j.ebiom.2019.05.025>
- Shah, K. N., Bhatt, R., Rotow, J., Rohrberg, J., Olivas, V., Wang, V. E., . . . Bandyopadhyay, S. (2019). Aurora kinase A drives the evolution of resistance to

- third-generation EGFR inhibitors in lung cancer. *Nature Medicine*, 25(1), 111-118. <https://doi.org/10.1038/s41591-018-0264-7>
- Shostak, K., & Chariot, A. (2015). EGFR and NF- κ B: partners in cancer. *Trends in Molecular Medicine*, 21(6), 385-393. <https://doi.org/10.1016/j.molmed.2015.04.001>
- Sigismund, S., Avanzato, D., & Lanzetti, L. (2018). Emerging functions of the EGFR in cancer. *Molecular Oncology*, 12(1), 3-20. <https://doi.org/10.1002/1878-0261.12155>
- Soria, J. C., Ohe, Y., Vansteenkiste, J., Reungwetwattana, T., Chewaskulyong, B., Lee, K. H., . . . Investigators, F. (2018). Osimertinib in Untreated EGFR-Mutated Advanced Non-Small-Cell Lung Cancer. *New England Journal of Medicine*, 378(2), 113-125. <https://doi.org/10.1056/NEJMoa1713137>
- Tanese, K., Hashimoto, Y., Berkova, Z., Wang, Y., Samaniego, F., Lee, J. E., . . . Grimm, E. A. (2015). Cell Surface CD74-MIF Interactions Drive Melanoma Survival in Response to Interferon- γ . *Journal of Investigative Dermatology*, 135(11), 2775-2784. <https://doi.org/10.1038/jid.2015.204>
- Taniguchi, H., Yamada, T., Wang, R., Tanimura, K., Adachi, Y., Nishiyama, A., . . . Yano, S. (2019). AXL confers intrinsic resistance to osimertinib and advances the emergence of tolerant cells. *Nature Communications*, 10(1), 259. <https://doi.org/10.1038/s41467-018-08074-0>
- Thiele, M., Donnelly, S. C., & Mitchell, R. A. (2022). OxMIF: a druggable isoform of macrophage migration inhibitory factor in cancer and inflammatory diseases.

Journal for Immunotherapy of Cancer, 10(9). <https://doi.org/10.1136/jitc-2022-005475>

Wang, N., Liang, H., & Zen, K. (2014). Molecular mechanisms that influence the macrophage m1-m2 polarization balance. *Frontiers in Immunology*, 5, 614. <https://doi.org/10.3389/fimmu.2014.00614>

Wang, R., Yamada, T., Kita, K., Taniguchi, H., Arai, S., Fukuda, K., . . . Yano, S. (2020). Transient IGF-1R inhibition combined with osimertinib eradicates AXL-low expressing EGFR mutated lung cancer. *Nature Communications*, 11(1), 4607. <https://doi.org/10.1038/s41467-020-18442-4>

Zhao, S., Molina, A., Yu, A., Hanson, J., Cheung, H., Li, X., & Natkunam, Y. (2019). High frequency of CD74 expression in lymphomas: implications for targeted therapy using a novel anti-CD74-drug conjugate. *Journal of Pathology: Clinical Research*, 5(1), 12-24. <https://doi.org/10.1002/cjp2.114>

CURRICULUM VITAE

